

ESTABLISHMENT OF LITHO-STRUCTURAL
CHARACTERISTICS OF SIWALIKS IN KANGRA SUB
BASIN TO UNDERSTAND THE CONTROL OF URANIUM
MINERALISATION ALONG PANIALI – LOHARKAR –
GALOT TRACT, HAMIRPUR DIST, HIMACHAL PRADESH

by

ABHIJITH V.

ENGG1G201801011

Bhabha Atomic Research Centre, Mumbai

*A thesis submitted to the
Board of Studies in Engineering Sciences*

In partial fulfillment of requirements

for the Degree of

MASTER OF TECHNOLOGY

of

HOMI BHABHA NATIONAL INSTITUTE

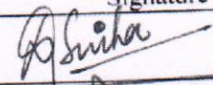
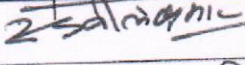
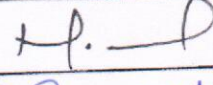
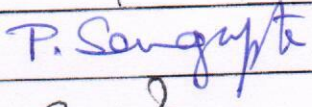
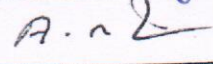
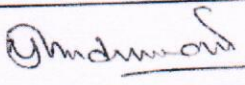
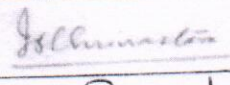
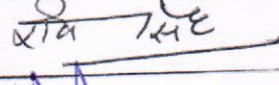
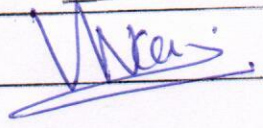


February, 2021

Homi Bhabha National Institute

Recommendations of the Thesis Examining Committee

As members of the Thesis examining Committee, we recommend that the thesis prepared by **Abhijit V** entitled "Establishment of Litho-structural characteristics of Siwaliks in Kangra sub basin to understand the control of uranium mineralisation along Paniali - Loharkar - Galot tract, Hamirpur dist, Himachal Pradesh" be accepted as fulfilling the thesis requirement for the Degree of Master of Technology.

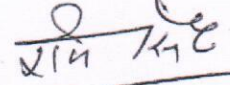
	Name	Signature
Member-1	Dr. D. K. Sinha	
Member-2	Dr. T. S. Sunil Kumar	
Member-3	Dr. Navin Goyal	
Member-4	Dr. Pranesh Sengupta ^s	
Member-5	Dr. A. Rama Raju	
Technical advisor	P. K. Sharma	
Examiner	Prof. J. P. Shrivastava ^s	
Guide & Convener	Dr. R. V. Singh	
Chairman	Prof. Vivekanand Kain ^s	

Final approval and acceptance of this thesis is contingent upon the candidate's submission of the final copies of the thesis to HBNI.

I hereby certify that I have read this thesis prepared under my direction and recommend that it may be accepted as fulfilling the thesis requirement.

Date: 15-02-2021

Place: Hyderabad


(Dr. R. V. Singh)
Guide



DECLARATION

I, hereby declare that the investigation presented in the thesis has been carried out by me. The work is original and has not been submitted earlier as a whole or in part for a degree / diploma at this or any other Institution / University.



(Abhijith V.)

DEDICATIONS

Dedicated to my family

ACKNOWLEDGEMENTS

First and foremost, I would like to express my gratitude towards Director, AMD for the opportunity to carry out this project work as part of M.Tech degree. I thank Dr. R.V.Singh, Regional Director South Central Region and my guide for his support and encouragement for carrying out the work. I am grateful to Shri, P.K. Sharma, technical advisor for his constant monitoring, suggestions and support during the course of the work. This project work has been actualized because of their support and encouragement while making sure that we get timely technical support.

I am very much grateful to Dr. Niranjana Kumar, for the technical and moral support he has provided as a field partner and senior colleague. His suggestions have been of great help in improving my work.

I am grateful to Dr. B.V.S.N. Raju, former RD, Northern Region, AMD, for the guidance and encouragement he has provided. His gestures of appreciation imparted confidence from the start of my project work.

Discussions and opinions from the side of The Director, AMD, Dr. D. K. Sinha, Shri. B. Saravanan, AD (Op-II), Shri. A.K. Bhatt, former AD (Op-II), Dr. T.S. Sunil Kumar, AD (R&D) have been very positive.

I am indebted to Smt. Sikta Patnaik and Shri. Somnath Bandyopadhyay for their timely cooperation and help in carrying out petrographic studies. Their willingness to help and provide microscope facility at any time is very much appreciated. Thanks are due to the officers and staff of Physics laboratory, AMD, Northern Region, New Delhi, XRF Laboratory, AMD, Central Region, Nagpur and Chemistry Laboratory, AMD, Jaipur.

I remember with respect the help extended by Shri. Keshav Ram, work assistant and Shri. K.K. Sharma, driver in carrying out the field work, despite the difficult terrain and conditions. Shri Jagannath and Amar Singh, technicians, also deserve a lot of gratitude for the help and service provided by them.

I am grateful to Shri. Vikram Jeet, Shri Rohit Kumar, Sh. Sumit Thakur and Sh. Karam Chand for their help in the field. I also thank the people of Nara, distt. Hamirpur, Himachal Pradesh for their heartwarming gestures during my stay in the field, especially during the COVID-19 lockdown period.

I thank my friend and colleague Shri. Subhajt Pandey for all his cooperation and

company during the limited stays in Delhi. I also thank Shri. Deepankar Sarma, for his cooperation and support in carrying out my project work along with the field assignment. I also thank Shri. Sushant Murmu, for providing moral support as a senior, during my difficult times.

Last but not the least, I thank my parents, my brother for boosting my morale up and for holding on together while I am away even during their difficult times. I also thank my wife who came along with me in between the course of the project and took all the burden of being the wife of a geologist.

CONTENTS

	Page
	No.
Synopsis	ii
List of figures	iv
List of tables	vi
List of Publications	vii
Chapter 1. Introduction	1
Chapter 2. Literature Review	10
Chapter 3. Methodology	13
Chapter 4. Geology of the area	18
Chapter 5. Results and Interpretation	34
1. Radiometric studies	34
2. Petrography	35
3. XRF Analysis	37
4. Carbon and Sulphur Analysis	41
Chapter 6. Discussion	42
Chapter 7. Conclusion	49
Future scope of work	50
References	51

SYNOPSIS

Lithostructural characterization of Siwaliks in Kangra subbasin has been carried out to understand the controls of uranium mineralization in the Paniali-Loharkar-Galot tract of Hamirpur dist., Himachal Pradesh. The Middle Eocene- Pliocene aged Siwalik Group of rocks, are represented in the study area by multi-storeyed stacks of sandstone, pebble beds and mudstone lenses dominantly of the Middle and Upper Siwaliks as well as the Middle-Upper Siwalik transition,. These are tectonically disturbed mainly by Jwalamukhi and Barasar thrusts and their associated synclinal structures and later faults formed by thrust propagation in the Himalayan Foreland Basin. Uranium mineralization occurs along the transition of Middle and Upper Siwaliks in this area. An integration of remote sensing, field work, radiometric survey, petrography and geochemical study using XRF analysis is employed to characterize the lithology, to generate the lithostructural map of the area and to understand the controls of uranium mineralization. Python programming was attempted to generate a 3D plot of field data. Structural and geomorphological lineaments identified in remote sensing include thrusts, faults, dipslopes, river escarpments etc., while geology is dominated by sandstone of sublithic to feldspathic litharenite composition showing color variation from buff to brown in vertical section. The sediment source ranges from granitic, volcanic, metamorphic and sedimentary rocks as revealed by petrographic. Geochemical studies suggest change of the source tectonic setting from passive to active continental margin upwards in the transition zone sediments, which may be related to tectonic activity along Main Boundary Thrust at about 5 Ma. The radioactive anomalies in the grey sandstone, associated with mud clasts, calcite- cemented lenses and carbonaceous matter, assayed 0.01- 0.28% U_3O_8 (n=17) and are dominantly associated with the carbonaceous matter and clay in the sandstone matrix, indicating adsorbed nature. The Masanbal - Biru- Paniali tract to the western part of study area shows pronounced variation in sandstone colour and radioactivity while a NW-SE trending reverse fault has

uplifted the stratigraphically lower horizons in the east along Loharkar-Galot tract, represented dominantly by grey sandstone which shows less colour variation but better continuity and order of radioactivity. The decrease in intensity of oxidation and the increase in order of radioactivity with depth as well as variations in sandstone and mud clast characteristics are also correlated. The study suggests that the oxidation of sandstones and remobilization of Uranium followed by the adsorption into clay and carbonaceous matter in the relatively reduced zone in grey sandstone dominantly resulted in the mineralisation. Continued tectonic activity within the Himalayan Foreland Basin is found to have disturbed the stratigraphy and thereby the mineralisation on a later stage.

Keywords: *Siwaliks, sandstone, uranium, oxidation, Kangra sub basin, Himalayan foreland basin*

LIST OF FIGURES

Figure No.	Description	Page No.
1.1	Schematic diagram of foreland basin with different depozones from Einsele (2013) Modified after DeCelles and Giles (1996).	2
1.2	Stratigraphy of the Tertiary sediment sequence in Himalaya (Kothari et al., 2017)	3
1.3	Geological map of Himalayas in the Kangra subbasin area showing radioactive anomalies (Ghosh et al., 2017; Kothari, 2018)	7
3.1	Processing flow chart adapted for LISS III imagery processing	14
4.1	(a) Limonitic light brown sandstone with oxidation haloes around mud clasts in Paniali (b) Light grey sandstones with basal pebbles near Biru (c) Light grey sandstones with whitish appearance near Sureri (d) Lithological section along Paniali- Biru-Sureri area	22
4.2	Goethite banded sandstone (below) and limonitic banded sandstone above near Biru in which low order activity of 1.5-3xbg was recorded	23
4.3	Calclitic cemented lens with mud clast in grey coarse grained sandstone with radioactivity	24
4.4	Grey sandstones and pebble beds along stream section along Dadh Khad,	26
4.5	Lithological section along Dadh Khad stream section	26
4.6	(a) Reverse fault with fault plane dipping SW near Sukhar Khad (b) Fault zone in mudstone. Camera facing in NW direction	26
4.7	Grey sandstones and pebble beds along stream section along Dadh Khad, near Loharkar	27
4.8	Pebble beds with grey sandstone lenses along stream section, near Nalti	28
4.9	Secondary copper minerals associated with uranium mineralisation in Romehra	28
4.10	Lineament map generated from LISS III Imagery superimposed on FCC composite	29
4.11	Lineament map generated from Cartosat DEM superimposed on Shaded Relief Map	29
4.12	Lineament map generated from Cartosat DEM superimposed on Slope image derived from DEM	29

4.13	Lineaments in the study area identified during field work and ground verification.	32
4.14	Lower hemisphere equal area projections of synclinal structures associated with (a) Barsar Thrust (b) Jwalamukhi Thrust	33
4.15	Geological Map of the study area, superimposed on the Digital Elevation Model	33
5.1	Few selected photomicrographs (PPL) of nonradioactive samples from the study area	35
5.2	(a) Calcite (sparry) in lithic arenites (b) Matrix with clay and carbonaceous matter. Feldspar disintegration along grain boundary (c) Fe-oxide coating of quartz grains revealed in reflected light (d) carbonaceous matter in the matrix along with corresponding α -track.	36
5.3	(a) Matrix with clay and carbonaceous matter with corresponding α -track. (b) and (c) Framboidal pyrite seen at higher magnification in oil immersion. The outer rim shows evidence of oxidation.	37
5.4	Plot of $\log (\text{Na}_2\text{O} / \text{K}_2\text{O})$ vs $\log (\text{SiO}_2 / \text{Al}_2\text{O}_3)$ after Pettijohn et al., (1987) for geochemical classification of sandstones	38
5.5	TiO_2 vs Al_2O_3 plot for discriminating the source rock characteristics	39
5.6	$\text{Na}_2\text{O} / \text{K}_2\text{O}$ vs SiO_2 diagram of Roser and Korsch (1986).	39
5.7	(a) $\text{SiO}_2 / \text{Al}_2\text{O}_3$ vs $\text{K}_2\text{O} / \text{Na}_2\text{O}$ diagram of Maynard et al. (1982) <i>PM</i> Passive Margin, <i>ACM</i> Active Continental Margin (b) ternary plot of $\text{SiO}_2 / 20 - (\text{Na}_2\text{O} + \text{K}_2\text{O}) - (\text{TiO}_2 + \text{Fe}_2\text{O}_3 + \text{MgO})$ (after Kroonenberg, 1994). <i>A</i> Oceanic island arc, <i>B</i> continental island arc, <i>C</i> active continental margin, <i>D</i> passive margin	40
6.1	A representative 3D block diagram based on interactive plot generated from GPS based field data along with geological and structural information. The dots represent data points in the 3D space, with red dots corresponding to surface anomalies. Orientation of the block with respect to north direction was decided based on the suitable viewing angle generated from the interactive plot.	44
6.2	Representative diagram showing the variation in the redox condition of mud clasts, sandstones and radioactivity with increasing depth.	45

LIST OF TABLES

Table No	Description	Page No.
5.1	Table showing the physical assay results of radioactive samples from Masanbal and Nalti area, Dist. Hamirpur, H.P.	34
5.2	Table showing the results of carbon and sulphur analysis of samples from Paniali- Loharkr-Galot tract, Dist. Hamirpur, H.P.	41

LIST OF PUBLICAITONS

Sl.

Paper Title

No

1. Integrated exploratory approach to the litho-structural characterization of Siwaliks in Kangra sub basin- A case study from the uranium mineralized Paniali- Loharkar-Galot tract, Hamirpur distt., H.P.*

Journal : Journal of The Geological Society of India[#]

*Publication being drafted and the title is subject to change

[#] Prospective, may change based on acceptance

CHAPTER 1

INTRODUCTION

Studies in parts of the Siwalik basin are carried out currently for establishing the possible litho-structural controls for the U mineralisation. Earlier exploratory works of the department beginning in the year 1970s through to 1990s yielded significant uranium mineralisation with the host rock mainly identified as sandstone and mudstone.

The Middle Eocene to Pliocene (18.3 – 0.2 Ma) Siwalik basin is a multi-storeyed molasse sedimentary sequence of fluvial origin in the Himalayan Foreland Basin (HFB), intersected by a network of thrusts, associated folds and cross faults (Dubey, 2014). The lithostructural setup of Siwalik basin is favourable for sandstone hosted uranium mineralisation, which is already identified in different parts of the basin, though not restricted to sandstones. Primarily lithological controls of mineralisation have been proposed (Kaul et al., 1993; Ghosh et al., 2017; Rahaman et al., 2017) and this study explores the role of structures in controlling the mineralisation.

Foreland basins, including the Himalayan Foreland Basin owe their formation to flexural bending and thrusting associated with collisional mountain ranges (Figure 1.1.) from where the sediments are supplied by weathering and erosion of the crystalline rocks of the hanging wall block. These basins form elongate depressions of hundreds to thousands of kilometres length (e.g. HFB >2500 km long and 200-300 km wide) between a thrust belt and adjacent cratonic region(s) and may derive sediments from both regions (Schwab, 1986; DeCelles and Hertel, 1989; Critelli and Ingersoll, 1994; DeCelles and Gilles, 1996). Based on the locations of sedimentation with respect to the thrust belt, different depozones (Figure 1.1.) are identified in a basin, namely wedge top, foredeep, forebulge and backbulge (Allen and

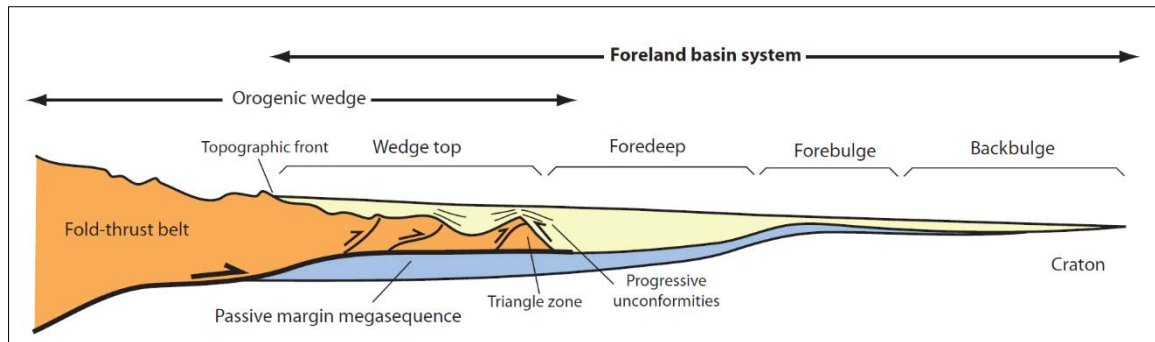


Figure 1.1 Schematic diagram of foreland basin with different depozones after Einsele (2013)

Allen, 2013) and the sediment characteristics are controlled by the shift in the depozones due to the subsidence of basin under topographic or sediment load. An initial flysch sedimentary sequence gradually transitions into a molasse sequence (Miall, 2000). Siwalik basin formed towards the later stage of thrusting along the Himalayan fold-thrust belt with sediment supply from the weathering and erosion of Early Proterozoic to Cretaceous rocks of the Higher and the Tethyan Himalayan tectonic units (Crawford, 1974; Valdiya, 1970, 1980; Valdiya et al., 1984; Valdiya, 1989; Brown and Nazarchuk, 1993; Raiverman, 2002) along with the Cenozoic sediments within the Sub-Himalayan tectonic unit (Raiverman, 2002).

The propagation of the main thrusting results in syn and post sedimentary deformation in the foreland basins, which in turn results in the widening of the fold-thrust belt (Dahlstorm, 1970; Miall, 2000). Within basin faults develop and propagate from below the basin, cutting through and uplifting the basin sediments (Miall, 2000). The continued faulting and folding results in the formation of synclines, anticlines and faults at different scales within the basin (Dubey, 2014). Syn-sedimentary deformation may also result in the formation of minor basins and sub basins bounded by cross faults. The Kangra basin is a sub basin formed within the Siwaliks.

1.1 Geology of the Siwalik Group

The Siwalik sediments overlay the marine sediments of the Subathu and fluvial sediments of Dharamshala Group in the HFB. The stratigraphic succession of the Siwaliks (Kothari et al., 2017) is shown in Figure 1.2.

The Lower Siwaliks are divided into Kamliak and Chinji Formations of fluvial sediments (Pilgrim, 1910). The Kamliak Formation consists of fine to medium grained, soft to well indurated greyish sandstone, occasionally brownish sandstone and purple shale (Johnson et al., 1985; Raiverman, 2002). Mammalian fossil assemblage suggest Middle Miocene age

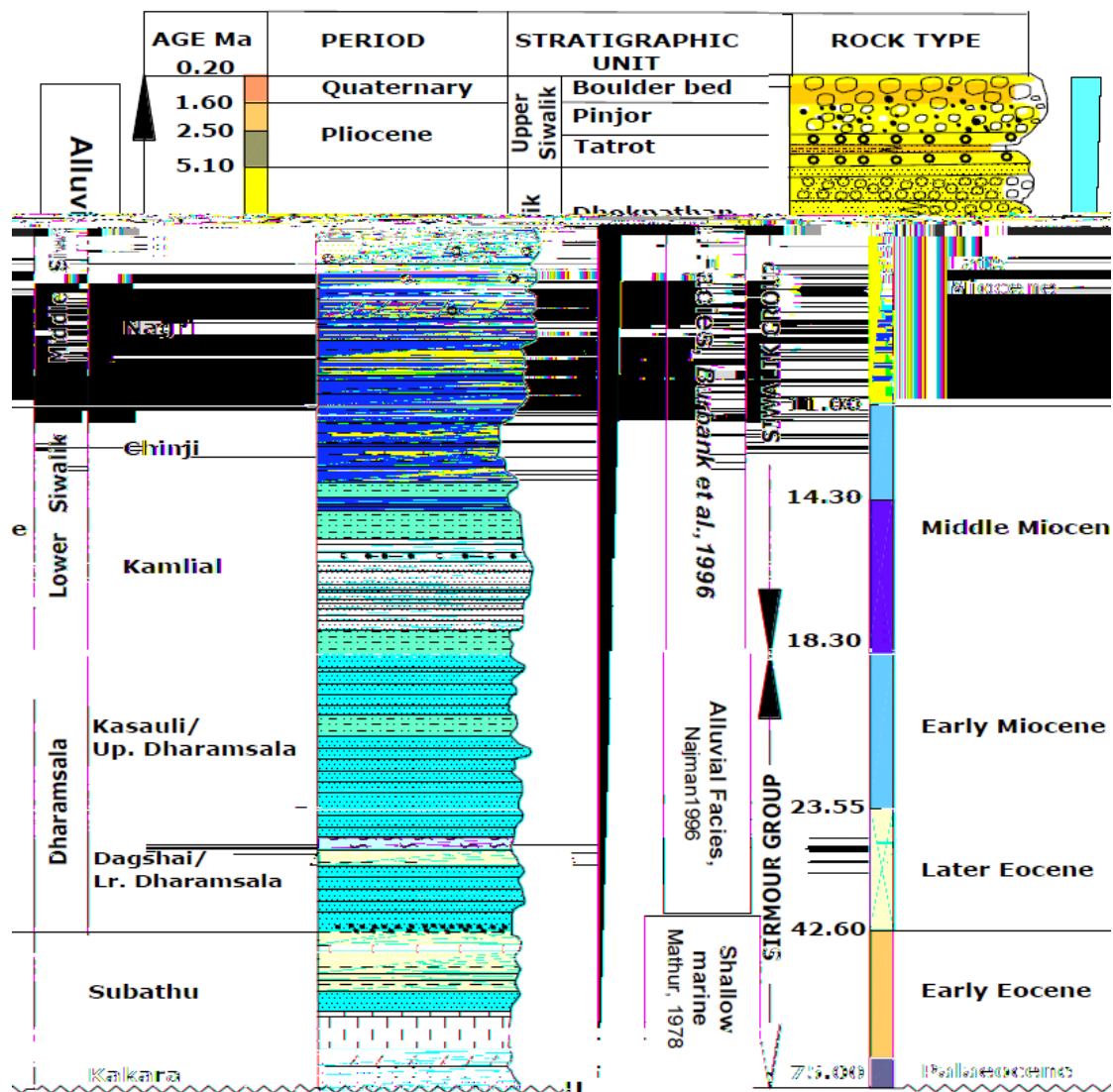


Figure 1.2 Stratigraphy of the Tertiary sediment sequence in Himalaya (after Kothari et al., 2017).

(Pilgrim, 1913) while magnetostratigraphy suggests an Early to Mid. Miocene (18.3 - 14.3 Ma) age (Johnson et al., 1985). The Chinji Formation consists dominantly of brown and yellow claystone with subordinate amounts of grey and brown sandstone. Vertebrate fossil assemblage suggests Mid. Miocene age (Pilgrim, 1910; 1913), while magnetostratigraphic age is determined to be Mid. to Late Miocene (Johnson, 1985).

The Middle Siwalik subgroup consists of Nagri and Dhokpathan Formations, which are consisted dominantly of sandstones with subordinate amount of clay and conglomerates. Grey to greenish grey, medium to coarse grained, friable sandstone with hard lenses of carbonate cemented layers. Subordinate amounts of brown to grey silty claystone and conglomerate with pebble sized clasts of igneous rocks and limestone are also present. Vertebrate fossil assemblage and magnetostratigraphic age suggests Late Miocene (10.8- 8.5 Ma) age (Pilgrim, 1910; Pascoe, 1964; Johnson et al., 1985).

Dhokpathan Formation consists of light grey to white, friable, calcareous sandstone with occasionally brownish grey sandstone. Dull red and orange coloured claystone and conglomerates are present in subordinate amounts. An Early Pliocene age from vertebrate fossil assemblage (Pilgrim, 1910; 1913) and Late Miocene (7.9- 5.1 Ma) age from magnetostratigraphy are suggested (Johnson et al., 1985). Clay content increases upwards in the Middle Siwalik. Sandstone contains dispersed pebbles of quartzites whereas the calcareous lenses can be identified as a characteristic feature of the subgroup.

The Upper Siwalik, rich in conglomerates, is divided into three formations namely Tatrot, Pinjor and Boulder Conglomerate Formations. The Tatrot Formation is composed of conglomerates, friable, grey, medium to coarse grained sandstone and clay varying from orange to brown in colour. The pebble clast composition of the conglomerate is dominantly metamorphic and igneous rocks along with Mesozoic to Tertiary sedimentary rocks. Vertebrate

fossil assemblage suggests Middle Pliocene age while magnetostratigraphic age is determined to be 5.2 – 2.5 Ma (Pilgrim 1910; 1913; Tandon et al., 1984; Sangode et al., 1996).

The Pinjor Formation consists of coarse, light grey to white sandstone and light pink siltstone. Early Pleistocene age is suggested by vertebrate fossil assemblage (Pilgrim, 1913). The boulder conglomerate, the youngest formation consists of conglomerates with clasts of igneous metamorphic and sedimentary rocks. The pebble composition varies from quartzite dominated in the oldest to limestone in the middle to mixed composition in the upper part (Pilgrim, 1913; Raiverman, 2002).

Structurally, the Sub- Himalayan tectonic unit, to which the Siwaliks belong, is bounded by the Main Boundary Thrust (MBT) to the north, which separates it from the Lesser Himalayas and the Main Frontal Thrust to the south, which separates it from the Indo-Gangetic foredeep (Raiverman, 2002). The Cenozoic sedimentary sequence in this unit is divided by the Main Boundary Fault- MBF (Medlicott, 1865) into a parautochthon consisting of Palaeogene sediments and an autochthon consisting of Neogene to Quaternary sediments of the Siwalik Group (Boileau and Kohli, 1952; Raiverman et al., 1993; 1994b). Subsidiary thrusts, namely Nalagarh Thrust, Soan Thrust, Barsar Thrust, Jwalamukhi Thrust and Palampur Thrust dissect the Siwaliks from its southern to northern boundary. The zone bound by Barsar and Jwalamukhi thrusts are found to be tectonically most active in the basin. The weakly deformed Siwalik rocks have developed macroscopic noncylindrical folds; the fault bend or fault propagation folds exposed near the thrusts and buckle folds away from the thrusts, where there is less shear strain (Raiverman, 2002). The large scale thrust are accompanied by younger strike slip faults and normal faults of small magnitude. Fault traces along major fold hinge lines indicate that they have formed during folding. Back thrusts have formed at a later stage of foreland propagation of the major thrusts (Dubey, 2014).

1.2 Mineral Potential of Foreland basins and Uranium mineralisation in the Siwaliks

The structural and sedimentary architecture of foreland basins make them potential hosts of variety of mineral deposits and hydrocarbon resources. The vast network of thrusts, faults and cross faults may aid in circulation of mineralised fluids across different parts of the basin, by forming a plumbing system. The molasse sediment sequences provide sufficient permeability for these fluids to invade and circulating meteoric water systems help set up redox fronts whereas confinements of sedimentological and structural nature may facilitate entrapment and preservation of the mineralisation. Oliver (1986) proposed that the fluids that are expelled out of the basin sediments below the thrust sheets may effect the faulting, metal transport, hydrocarbon migration or even metasomatism within the vicinity. As postulated by Leach et al. (1984), Mississippi Valley-type lead-zinc deposits of the central United States were deposited from hydrothermal fluids that were expelled from Ouachita foreland basin.

The multi-storeyed sedimentary sequence of sandstone, conglomerate and occasional clay as well as calcitic cementations, make the Siwaliks suitable lithostructural locale for hosting uranium mineralisation in the redox interfaces as well as in adsorbed form in the carbonaceous matter, iron hydroxides and clay. The uranium mineralisation is associated with the upper part of Lower Siwaliks as well as with the upper part of Middle Siwaliks- along the transition of Middle to Upper Siwalik. The mineralised horizons occur at the redox interfaces of oxidised and reduced sandstones, dominantly adsorbed in clay in the matrix, mud clasts and organic matter, while also being associated with calcite cemented lenses at places. Uranium mineralisation is also associated with the matrix component of pebble beds in the Middle Siwalik as well as with the mudstones of Lower Siwaliks. Figure 1.3. shows the geological map of the Kangra sub basin area with radioactive anomalies.

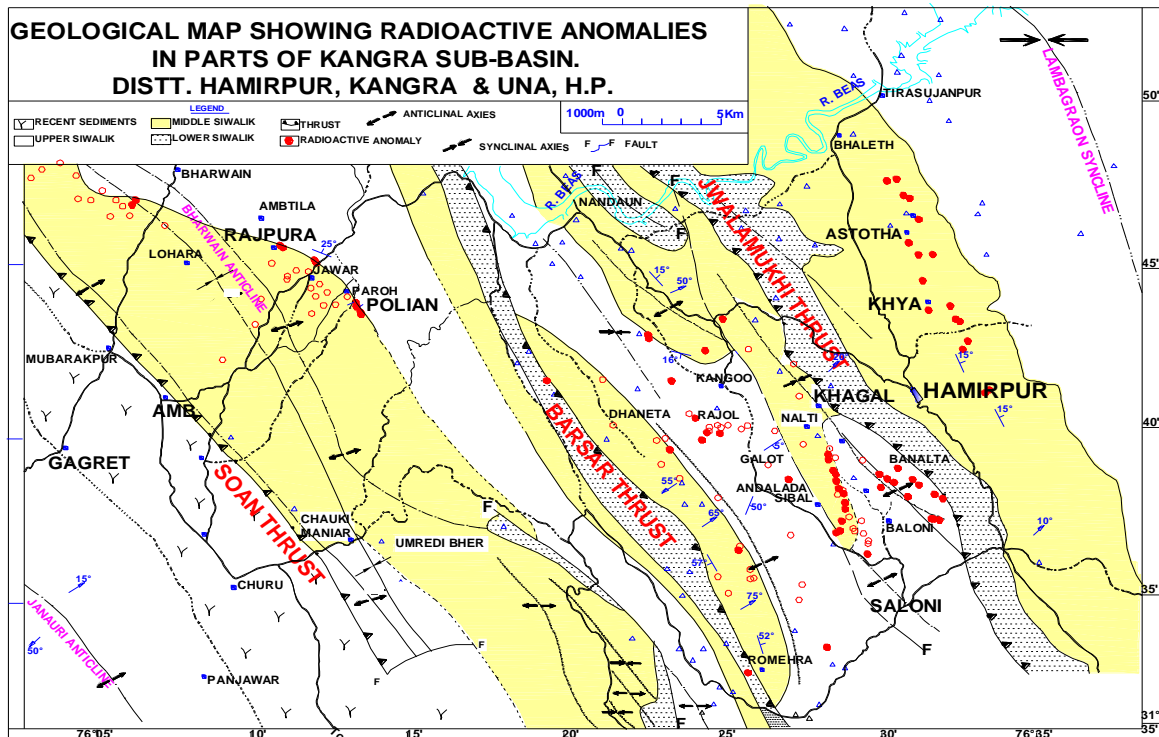


Figure 1.3 Geological map of Himalayas in the Kangra sub basin area showing radioactive anomalies (after Kothari, 2018)

Numerous studies have been attempted to understand the genetic aspects and controls of the uranium mineralisation in the Siwaliks. Though in literature the mineralisation is mentioned as ‘sandstone-hosted uranium mineralisation’, it is not restricted to the sandstone horizons and a one to one correlation with any of the sediment characteristics has not been established. Earlier studies by AMD (Ghosh et al., 2017; Rahaman et al., 2017; Kothari et al., 2019) propose that the uranium mineralisation in Siwaliks is lithologically controlled and is presently in dynamic state. Another factor which requires attention is the structural architecture of the basin, which consists of major subsidiary faults of the Himalayan fold- thrust belt, as well as anticlines, synclines, minor faults and cross faults. Along with these, lensoidal bedding, warping, within basin slips, slumps and other syn-sedimentary deformation structures put together may form an extensive network, which can transport mineralising solutions from below the basin and circulate it within the basin. The sedimentary and structural architecture provide entrapment mechanisms where uranium mineralisation can occur under favourable

physicochemical conditions (Moghal, 2001). During sedimentation and diagenesis, tectonic activity (neotectonics) may help remobilise and concentrate uranium in a lithostructurally controlled locales. Systematic studies in the uranium mineralised Siwaliks in the Kangra sub basin would aid in examining the relationship between the structures and uranium mineralisation. The regional structural pattern has to be delineated and studied alongside lithological variations, uranium mineralisation and host rock characteristics.

The study area, Paniali – Loharkar- Galot tract falls in the Kangra sub basin and is bounded by two thrusts : Barsar thrust to the southwest and Jwalamukhi thrust to the northeast. This tract, where Middle Siwalik sediments are dominantly exposed, along with Upper and Lower Siwaliks, is a promising area with ongoing exploration activities of AMD for uranium mineralisation since early 1970s. Geological, geophysical and geomorphometric studies indicate that the Barsar and Jwalamukhi thrusts and the zone bounded by them comprise the most active zone in the Kangra sub basin (Powers et al., 1998; Malik and Mohanty, 2007). Barsar thrust is a backthrust with fault plane dipping towards SW. Associated with these thrusts are two synclinal structures, Balaru syncline to the NE of Barsar thrust and another syncline to the SW of Jwalamukhi thrust. Presence of cross faults have also been mentioned in earlier studies.

Mineralisation in parts of this area and its surroundings is associated with grey and brown sandstone, matrix part of conglomerates and in mudstones of Dad Khad, Loharkar, Nalti and Romhera areas (Ghosh et al., 2017; Rahaman et al., 2017). With this preliminary information, studies are planned to establish the lithostructural characteristics favouring uranium mineralisation in this part of the basin.

1.4 Objectives

1. To identify, map and study the structural features in the Paniali- Loharkar- Galot tract of the Kangra sub basin to understand the structural pattern of the area at a scale of 1:25,000.
2. To characterise the lithologies, host rocks for uranium mineralisation and the nature of mineralisation.
3. To study the relationship between the distribution of uranium mineralisation and the regional structural pattern.
4. To develop a model to understand the controlling factors of uranium mineralisation with respect to structural aspects of the basin.

1.5 Deliverables

1. Lithostructural maps of the Paniali - Loharkar - Galot tract of the Kangra sub basin delineating structural features over an area of 10 sq.km. at 1:25,000 scale.
2. Orientation data of structural features in the study area.
3. A proposal, regarding a suitable model for understanding the controlling factors of uranium mineralisation with respect to structural aspects of the basin.

CHAPTER 2

LITERATURE REVIEW

The interdisciplinary study emphasising on all the processes that are involved in remobilising the element(s) of interest from the source, its transportation and concentration through segregation under conducive physico-chemical conditions and preservation through geological history to form a mineable ore deposit, is the modern day mineral exploration strategy. This is defined as mineral systems approach and was introduced by Wyborn et al., (1994).

The fundamental principles of sedimentary basin analysis, with the detailed description of formation, sedimentation history and tectonics of foreland basins are discussed by Einsele (2013), Allen and Allen (2013), Schwab (1986), DeCelles and Hertel (1989), Critelli and Ingersoll (1994) and DeCelles and Gilles (1996). Miall (2001) gives a comprehensive description of the Himalayan Foreland Basin.

Stratigraphic studies in the Siwalik were carried out by several authors including Pilgrim (1910; 1913), Pascoe (1964), Johnson et al. (1985) and the fossil assemblage based ages were determined by Pilgrim (1910; 1913) while Pascoe, (1964), Johnson et al., (1985) determined the magnetostratigraphic ages of the individual subgroups within the Siwalik Group. Geological Survey of India (GSI) and Oil and Natural Gas Corporation (ONGC) have carried out extensive stratigraphic studies for the exploration of minerals and hydrocarbon.

Geological Quadrangle map, with regional geology and major structures of the area was available from GSI web portal. A digitised district resource map as well as lineament map on 1:50,000 scale were accessed from the Bhuvan portal of National Remote Sensing Centre (NRSC). Raiverman (2002) presents a detailed study of the stratigraphy, structure and the evolution of the Himalayan Foreland Basin with energy sequence (enseq) concept. Mallik and

Mohanty (2007) studied the neotectonics of the terrain and delineated zones of neotectonics activity through morphotectonic studies based on satellite remote sensing.

Relevant inhouse data pertaining to the uranium exploration in Siwaliks since early 1970s were referred for the present study.

Annual reports, maps and toposheets were collected from the regional library and cartography section. Kaul et al. (1993) provides a comprehensive review of findings from the exploration activities carried out between early 70s to early 90s, with lithological descriptions, host rock characteristics, favourable physicochemical conditions, uranium mineralogy, and maps of delineated mineralisation on a regional scale.

The present study is intended towards understanding the controls of mineralisation with respect to the lithological and structural pattern, on a relatively detailed scale (1:25000). Similar studies by Osterwald and Dean (1961) established structural control on uranium mineralisation in the Cordilleean foreland basin.

The literature and information collected from Bhuvan portal of National Remote Sensing Centre (NRSC) included the digitised district resource map, lineament map on 1:50,000 scale.

Toposheet no. 53A/6 and 53A/10 pertaining to the area were collected from the cartography section. As proposed by Krishna et al. (2015) the publicly available IRS Resourcesat- 2 based LISS III imagery were found suitable for remote sensing studies of India. The Cartosat-1 based Digital Elevation Model (DEM) are suitable for the rugged terrains of Himalayan Region as referred by Baral et al. (2016).

The choice of Quantum GIS software (QGIS) were made for processing and management of geospatial data, with respect to geological mapping as discussed by Alshaghdari (2017) and Erharter and Palzer-Khomenko (2018). Kaul et al. (1993) suggested

that ground based radiometric surveys using in house developed instruments are most suitable method for studying uranium anomalies in field.

CHAPTER 3

METHODOLOGY

3.1 Literature Survey

A vast quantity of available literature in the form of published papers, books and earlier field season reports of Atomic Minerals Directorate for Exploration and Research (AMD) were studied for understanding the geological background, nature of mineralisation and to prepare basemaps from published maps. Literature related to remote sensing, processing of satellite imagery and Digital Elevation Model (DEM), structural studies on foreland basins, along with literature and online resources related to Quantum GIS (QGIS) were also studied for formulating the methodology for carrying out the project work.

3.2 Preparation of basemap

An integrated basemap was prepared by digitising and georeferencing existing maps which include : (i) Toposheets (no. 53A, 53A/6 and 53A/10) of the study area, collected from the cartographic section at Northern Region Headquarters, AMD, New Delhi. (ii) Published geological maps of Geological Survey of India (GSI) available in the online portal of GSI and (iii) Digitally available maps from Bhuvan portal of National Remote Sensing Centre (NRSC) (iv) Google Earth and ArcGIS Imagery

3.3 Remote sensing studies

Identification of structural features in a sedimentary terrain with loosely indurated or friable sediments has to be aided by toposheet and remote sensing based geomorphological studies. In this regard, Remote sensing studies were carried out for lineament identification, studying topographic features and variations etc., so as to prepare thematic layers in the database.

3.4 LISS III Imagery

IRS Resourcesat-2 LISS III imagery with 23.5 m spatial resolution and 10 bit radiometric resolution were used in lineament extraction. These imagery containing information in 4 spectral bands - Bands 2 to 4 in VNIR (0.52 - 0.86 μm) and Band 5 in SWIR (1.55 - 1.70 μm) - are available in already georeferenced and orthorectified format from the Bhuvan portal. Imagery pertaining to the local summer season were collected so as to have minimum vegetation cover in the images.

The processing algorithm of lineament extraction was designed accordingly as adapted from Hassan et al. (2014), Takorabt et al. (2018). The flowchart of image processing is shown in the figure 3.1. The georeferenced and orthorectified imagery was subsetting for the study area. The processing involved contrast enhancement by histogram enhancement, principal component analysis followed by directional sobel filtering lineament extraction.

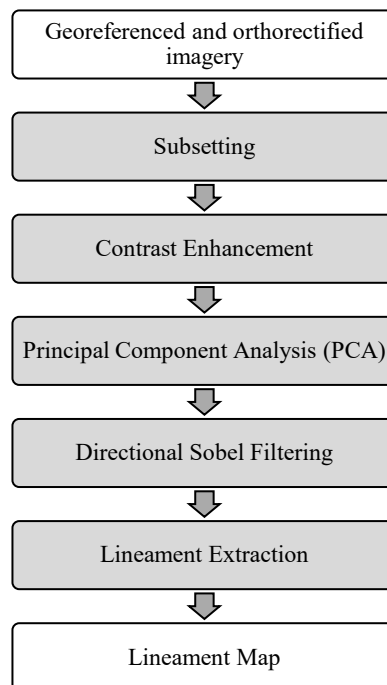


Figure 3.1 Processing flow chart adapted for LISS III imagery

3.4 Digital Elevation Model

The digital elevation model of the area was obtained from Cartosat-1 DEM derived from stereo pair pan imagery and having a spatial resolution of 30m. Topographic contour maps, shaded relief map and topographic profile were prepared using the DEM. The DEM was also used for 3D visualisation of the terrain with overlays of different layers. The superiority of Cartosat DEM over ASTER and SRTM based DEMs in rugged terrain is discussed by Baral et al. (2016).

3.5 Other available maps

Maps of district resources, landuse, drainage and lineaments (1:50,000 scale) etc., were incorporated from the Bhuvan portal of National Remote Sensing Centre (NRSC). Google earth and ArcGIS imageries were also used to prepare road network map and identification of lineaments.

3.6 Field work

Field work was carried out subsequently to remote sensing studies, for ground verification and geological survey and detailed mapping. Toposheets, DEM and lineament maps aided in planning the traverses. Lithological units at exposures were demarcated and geological sections were prepared. Structural data pertaining to beddings, fractures, joints, faults etc were collected and recorded systematically.

3.7 Radiometric survey

Radiation Survey Meter (RSM) was used to carry out radiometric survey on all exposures, to measure the surface gamma ray activity (in ppm eU_3O_8) of the rocks. The background values of radioactivity for each lithounit was determined and anomalous values were identified for detailed mapping and sampling.

3.8 Map preparation

Lithostructural map of about 10 sq.km. area in the Paniali-Loharkar-Galot tract was prepared, on a scale of 1:25000. Basemap was prepared by locating villages and towns using digitized and georeferenced toposheet, by tracing road and stream networks from digitally available georeferenced satellite imagery (Google earth, Open street map). Field data was plotted on the map using GPS and toposheet based location data. Thematic layers were prepared for lineaments extracted from LISS III imagery, lineaments extracted from DEM, geological map, structural data and radioactive anomalies. All maps and imagery were georeferenced to Geographic (Lat/Long) coordinate system, with WGS84 datum.

3.9 Sampling

Lithological grab sampling was carried out along the study area, where the exposures are limited to stream and road cutting sections. Samples were numbered systematically and sample slips were prepared, with field information as well as location data. Radioactive and non radioactive samples were collected separately and were sent for petromineralogical and gamma ray spectrometric studies to respective laboratories at NR headquarters, AMD, New Delhi. The samples are sent to petrography lab to carry out studies related to clast composition, texture, matrix, cement, radioactive phases, alterations if any and mineral paragenesis.

3.10 Software used

The free and open source QGIS (Quantum GIS) platform (QGIS 3.8.3 Zanzibar) was used for the organisation, management and analysis of geospatial data involved in this study. Within the project database, separate layers were prepared for lithological and lineament maps, plotting of structural information and radioactive anomalies. Plenty of tools, plugins and utilities available in QGIS were also used for collection and processing of data. This involved digitization of publicly available geospatial data provided by Google, Bhuvan portal of NRSC,

ArcGIS Imagery, Openstreet map etc., organisation of georeferenced satellite imagery and toposheets in raster format, preparation of digitized vector data of road and stream networks, lithology and point data such as radioactive anomalies and structural data, collection of orientation data of lineaments etc.

The lithological sections were prepared using AutoCAD software. The satellite imagery processing was carried out using ERDAS Imagine and GRASS. Programming in Python language was also carried out as part of an attempt to generate a 3D visualisation of the geological and structural data.

CHAPTER 4

GEOLOGY OF THE AREA

The study area, Paniali-Loharkar-Galot tract falls in the Kangra sub basin of the Siwalik basin and is bounded by Jwalamukhi thrust to the north and Barsar thrust to the south. The area taken up for the survey and mapping (1:25000 scale) include a 10 sq. km. block, with its adjoining 20 sq.km. area enclosed between 31° 37' 00" and 31° 40' 00" latitudes and 76° 24' 25" and 76° 30' 00" longitudes in toposheets no. 53A/6 and 53A/10.

Established stratigraphy of this area suggest that the rocks of Middle and Upper Siwalik constitute the dominant lithology, bound by the two thrusts along east and west. Observations made during the course of the present study are described in this chapter.

During the course of present studies lithological and structural data were recorded from road and river sections exposing sandstone, pebble beds and mudstone of varying characteristics. Attitude of beds tend to vary from horizontal to gentle to steep dips in opposite directions, with a general NW-SE strike. Within basin slip faults, joints etc. were also recorded at places. Radioactivity for individual units were recorded for determining the background values of the units and to identify anomalies. Spotty and patchy anomalies were recorded in different horizons, with widely ranging activities. Representative sampling was carried out for petromineralogical and radioelemental studies for lithological characterisation of the rock units. The following observations and recordings are made on 1:25000 scale.

4.1 Major lithounits

Sandstone, pebble beds and minor amounts of mud beds dominate the lithology of the area. Besides this, variations in the sandstone colour has also been observed. The descriptions of individual lithounits are given below.

4.1.1 Pebble beds

Pebble beds in the study area, limited to few exposures, occur as (i) the uppermost unit and as (ii) intraformational lenses. In both types, clast composition consist of pink and white quartzites, granitic gneisses and of indurated Fe-Mg rich mud clasts, which are dominantly of cobble size, with occasional pebble and boulder sized clasts. Pebble beds forming the uppermost units compose of matrix of reddish soil with clay, which suggests that they may be part of recent alluvium or soil. The intraformational pebble bed lenses tend to be supported by sandy matrix, with medium to coarse sized clasts. They form 6 - 7 m thick lenses with upto 40 m in the longer dimensions. The pebble beds are well exposed along the section near Masanbal, where the matrix show variations from yellowish (limonitic) to buff colour whereas the clasts of Fe-Mg rich indurated clay show corona structures interiorly and coating of bluish grey Fe oxides exteriorly, giving a metallic lustre (specularite-like) to the clasts. These features are indicative of oxidising environment. Significant radioactivity was not encountered in the pebble beds within the present study area, whereas in the adjoining Nalti area to the east, within the matrix component of pebble beds, significant radioactivity was recorded in earlier studies carried out by AMD.

4.1.2 Buff sandstone

Buff coloured sandstone is dominantly found in the southern part of the study area, in Paniali, Sureri and Balloh. These sandstone is medium to coarse grained, moderately sorted and consists of quartz, altered feldspar, clasts of Fe-Mg minerals and mica. Pebbles of quartzite and vein quartz are often found aligned along foresets of cross stratifications in this sandstone.

4.1.3 Limonitic Light Brown sandstone

In parts of Paniali, Sureri and Biru, limonitic light brown coloured sandstones are observed. This is dominantly medium to fine grained and consists of quartz, altered feldspar,

mica and iron hydroxide, which may be imparting the colour to the rock. Limonitic bands are observed in relatively less weathered surfaces exposed along recent road cuttings. Fe-Mg-Mn rich mud clasts of dark black to brown colour are found at certain sections, surrounded by rusty brown and black oxidation haloes of Fe and Mn. Radioactivity has also been recorded in these clasts.

4.1.4 Brown Sandstone

At places, especially near Tagoh, Balloh and Biru, brown sandstones is exposed and shows colour from orangish brown to reddish brown and are medium to fine grained with occasional clay content. The colour of the rock may be due to the presence of iron oxides and hydroxides (goethite gives orange colour). At certain places, banding is also observed.

4.1.5 Light Grey sandstone

In parts of Sureri, Manjrah and Biru and even westwards, light grey medium grained sandstone are exposed and contain less amount of Fe-Mg rich clasts and often contain patches of brown sandstone and limonitic sandstone with bandings. Mud clasts of dark grey to brown are present but are not found associated with haloes.

4.1.6 Brownish Grey sandstone

In sections near Masanbal, towards the upper part of the sections, brownish grey sandstones are exposed. These are medium to coarse grained and often contain lenses of grey mud and pebbly horizons. Activity of upto 2.5 xbg has been reported in the mud lenses within these units exposed near Biru.

4.1.7 Grey sandstone

The grey sandstone is the lowermost unit exposed in the study area, consisting of medium to coarse grained ill sorted sandstone with hard compact lenses with calcite cement.

Alongside that grey coloured clay, organic matter are also associated with the sandstone. This rock unit has dimensions – 2 km length along regional strike direction, 950 m width along dip direction and about 2 - 7 m thickness- and hosts the radioactive zone delineated, with values ranging from 50 ppm to 420 ppm as measured by radiation survey meter (RSM).

Grey sandstone is also exposed along the west and north of the area, from Pansai up to Bal, along the Maan Khad. But in this part, it is slightly greenish, medium to fine grained, with rare occurrence of calcitic cemented lenses, and tend to be more clayey. Clay lenses are also greenish grey and laminations are observed at places. In these parts, significant radioactivity was not encountered.

4.2 Area wise description of geology and radioactivity

4.2.1 Paniali

Exposures in Paniali area and its surroundings are restricted to road and stream sections, often along steep slopes and beneath high vegetation cover. The lithology consists dominantly of sandstone with exposures of conglomerate at places. Sandstone vary in color from grey to buff to yellowish and brown and is medium to coarse grained, moderately to ill sorted, and often pebbly. Compositionally these are arkosic-with feldspar often altered to clay minerals, micaceous- at places with both muscovite and biotite and often contain calcitic cemented lenses and mud clasts. Dark black minerals constitute about 5-20% of the mineralogy. The colour of the sandstone is dominantly yellowish grey to brown and fine limonitic banding is observed at places, suggestive of hydrous Fe oxides formed of near surface oxidation. Oxidation haloes with concentric ferruginous ring structures developed around a central dark brown core of mud is also observed within the sandstones in parts of Paniali.

To the south of Paniali, along Biru, Amroh and Sureri, light grey to limonitic light brown and brown sandstones dominate the lithology. These occur as coarse to medium grained

poorly to moderately sorted pebbly sandstones composed of quartz, feldspar, mica and dark black minerals. Light grey and grey sandstones show occasional limonitic banding and whitish colour (Figure 4.1). Basal part of individual beds are marked by pebbles while clast size tend to fine upwards within the beds (Figure 4.1d). Trough cross beddings defined by imbricated pebbles are also observed at places. Limonitic bandings and oxidation haloes are common in these sandstones. Yellowish to red 20-30 cm thick mud lenses are observed at certain places.

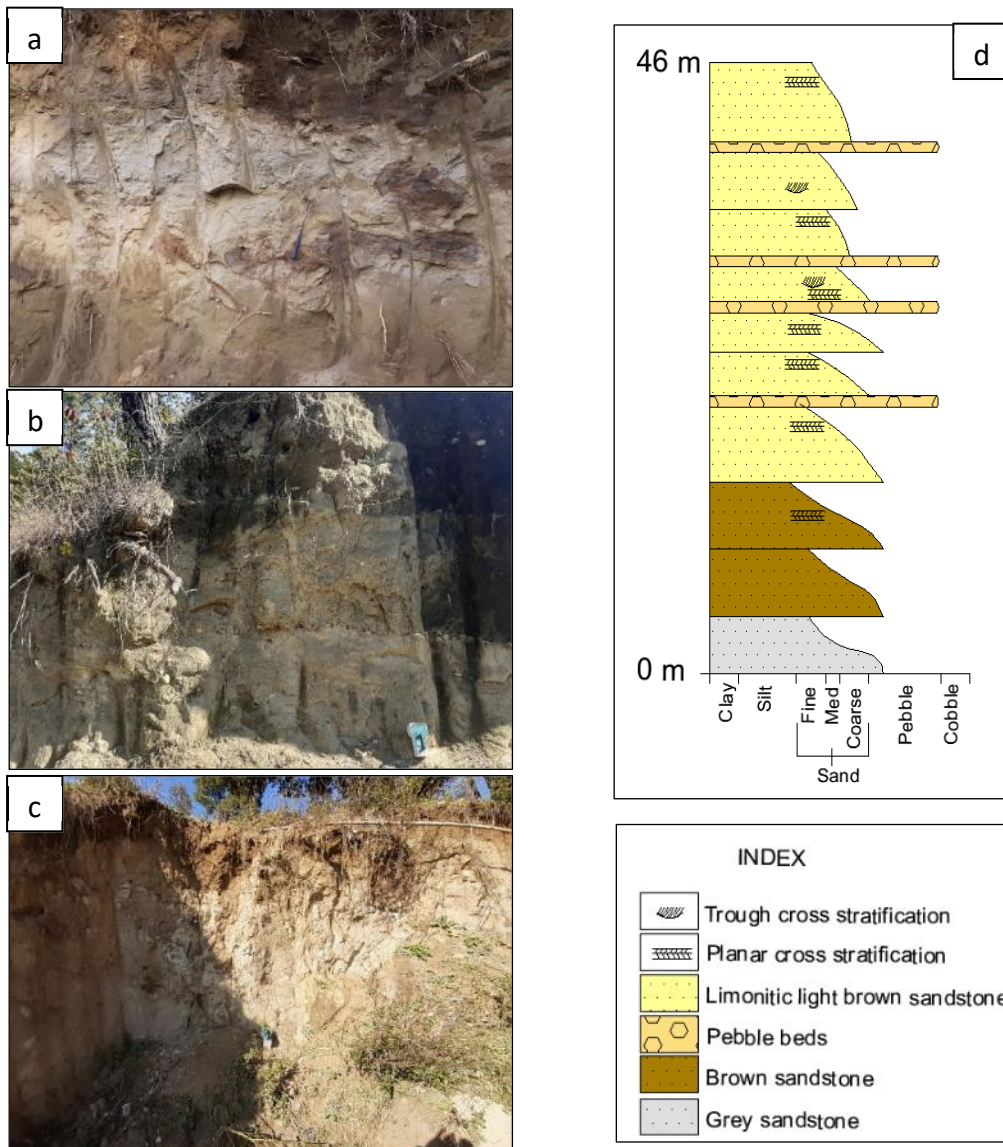


Figure 4.1 (a) Limonitic light brown sandstone with oxidation haloes around mud clasts in Paniali (b) Light grey sandstones with basal pebbles near Biru (c) Light grey sandstones with whitish appearance near Sureri (d) Lithological section along Paniali- Biru-Sureri area

Attitude of bedding plane measured in these sandstones is 145/18°W strike and dip respectively.

Along a north-south trending stream section, extending from Biru to Masanbal, spotty radioactivity ranging from 1.5-3xbg was recorded in yellowish limonitic and goethitic banded sandstone (Figure 4.2).

An anomaly of 1.5-2 xbg was recorded in brown mud clasts with oxidation haloes, with long dimension parallel to bedding and banding in limonitic banded yellowish grey sandstones (Figure 4.1a) along a road cutting section.



Figure 4.2 Goethite banded sandstone (below) and limonitic banded sandstone above near Biru in which low order activity of 1.5-3xbg was recorded

4.2.2 Masanbal

Greyish to buff to yellowish, medium to coarse grained sandstone and conglomerate are exposed along stream sections and road cuttings near Masanbal and Chorarah (Figure 4.3). Along Masanbal-Biru road section and Masanbal-Kangu road section, the conglomerates and sandstone are exposed. The section is dominated by conglomerates of pebble to cobble sized clasts and 1-3 m lenses of sandstone within the conglomerate (Figure 4.3). The conglomerate consists of white quartzite, pink quartzite, gneisses and mafic volcanics as clasts. The matrix is composed of sand to clay sized grains, of yellowish to reddish colour. Sandstone is composed of subangular to subrounded clasts of quartz, feldspar, mica and dark black minerals. The sandstone beds are marked by pebble horizon at the base and the clast size tend to fine upwards, within the beds. Calcitic cemented lenses are restricted to the sandstones in the lower part of the section. Within the sandstone lenses in conglomerates, trough cross beddings with foresets

marked by pebbles are observed. Bluish iron oxide coating is observed on the surface of mafic clasts in the conglomerates (Figure 4.3 b). Concentric ferruginous rings observed in the inside

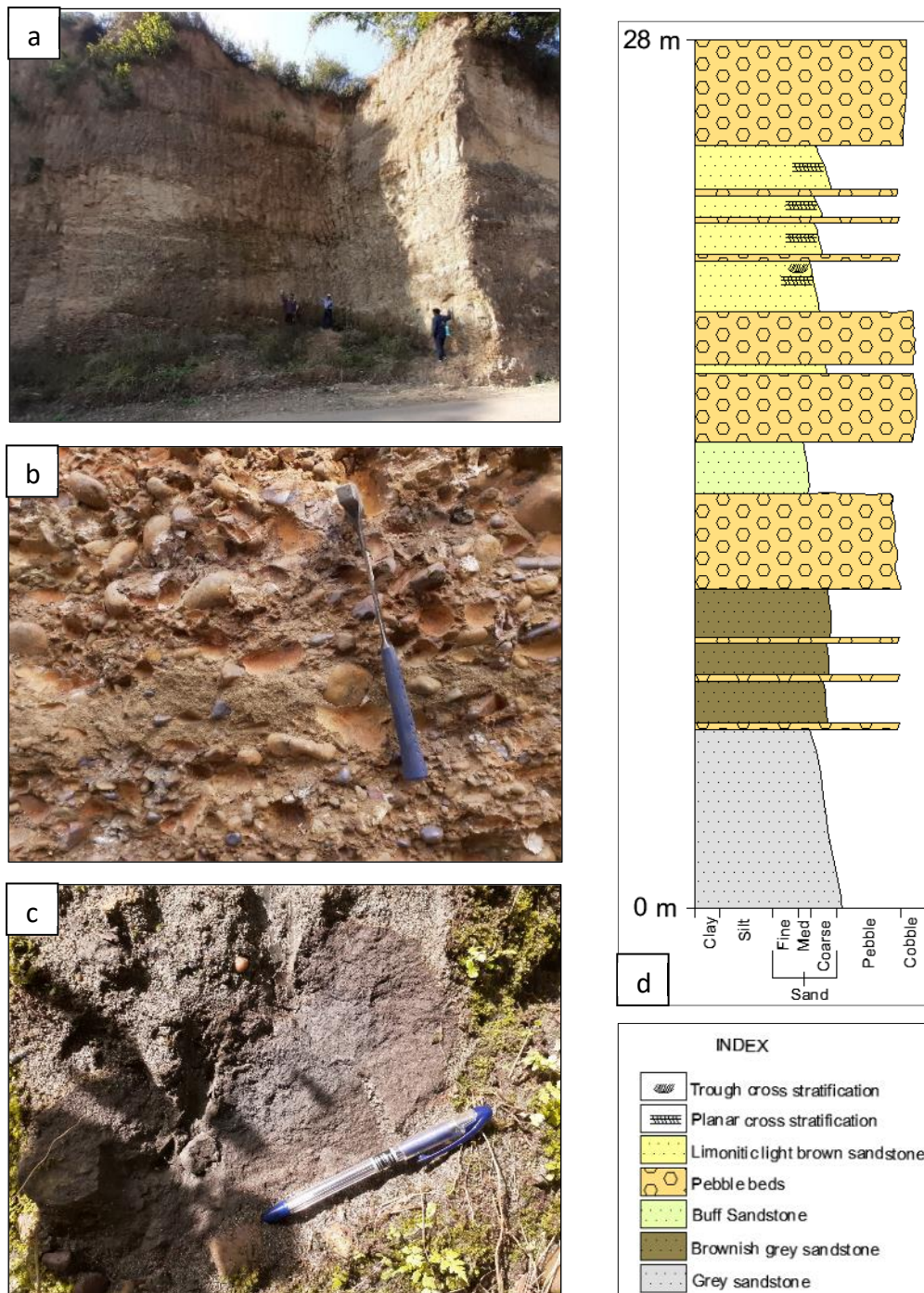


Figure 4.3 Calcitic cemented lens with mud clast in grey coarse grained sandstone with radioactivity

of these clasts indicate leaching of iron in the ferromagnesian minerals from the core of the clast to the surface.

The conglomerates are present as 1-2m thick lenses within the sandstone and as separate units of more than 7-8 m thickness as well. Wherever the conglomerates occur as thick separate units, they form the uppermost lithounit. The conglomerates are matrix supported, poorly sorted and consists of pebble to boulder sized clasts of white quartzite, pink quartzite, schists and greenish grey fine grained mafic rock clast (dolerite?) as well. The average clast size is of cobble size and the clasts generally show imbrications along flow direction. The matrix consists of yellowish brown to reddish clay to gravel sized clasts. Lenses of 1-2 m thick sandstone of yellowish to brown colour are present within these conglomerates.

Radioactivity of discontinuously patchy nature, encountered in the grey sandstone along the N-S trending river section to from Masanbal to Paniali has been traced to about 500 m long, 60-90 m wide and 2-7 m thick band with 50 ppm- 420 ppm values measured with RSM well above the background for the unit (15-20 ppm). The activity dies down to the north and to the south to about 30-20 ppm and eventually decreases to background. The activity is associated with calcitic cemented lenses, mud clasts, carbonaceous matter and Fe-Mn encrustations.

4.2.3 Galot – Loharkar - Nalti Tract

In the eastern part of the area, along Galot, Dadh Khad and Loharkar tract, southwest of Jwalamukhi Thrust, sandstones and pebble beds of Middle Siwalik are mapped.

4.2.3.1 Galot

Stream sections of Dadh Khad, Kunnah Khad and Sukhar Khad, along Galot-Sibal and Loharkar tract expose grey medium to coarse grained sandstone with conglomerate lenses (Figure 4.4). The dominant lithology present is grey sandstone, with pebbly horizons and 7-9 meters thick pebble bed lenses. The grey sandstone is medium to coarse grained, friable, poorly sorted and is composed of quartz, feldspar (often altered), mica, and dark, opaque minerals.

Sulphides are also present. At places, calcitic cemented lenses, parallel to the bedding, protrudes from the section. Pebble are aligned along the bedding plane within the sandstone at places. Lenticular structures present in the sandstone indicate braided



Figure 4.4 Grey sandstones and pebble beds along stream section along Dadh Khad,

channel features. About 7-9 meters thick and 35-40 meters wide lens of pebble bed is present in the section, bound above and below by grey sandstone (Figure 4.4, Figure 4.5). The beds of sandstone within the pebble bed lens define cross stratification. In the Dadh

Khad area, bedding planes of these rocks strike NNE-SSW with a eastward dip of 30-45°

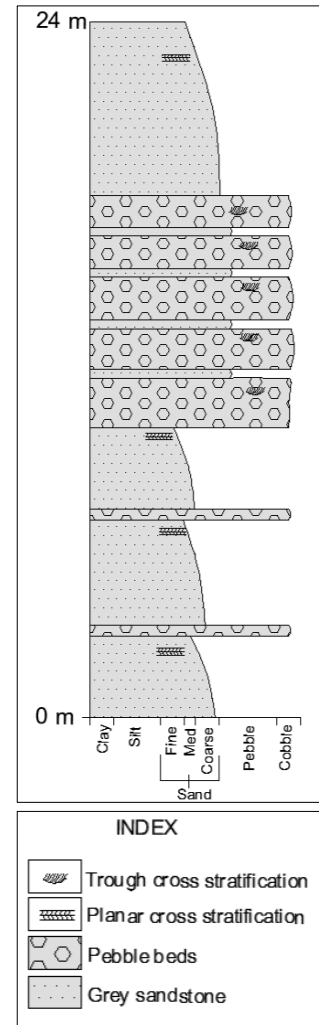


Figure 4.5 Lithological section along Dadh Khad stream section

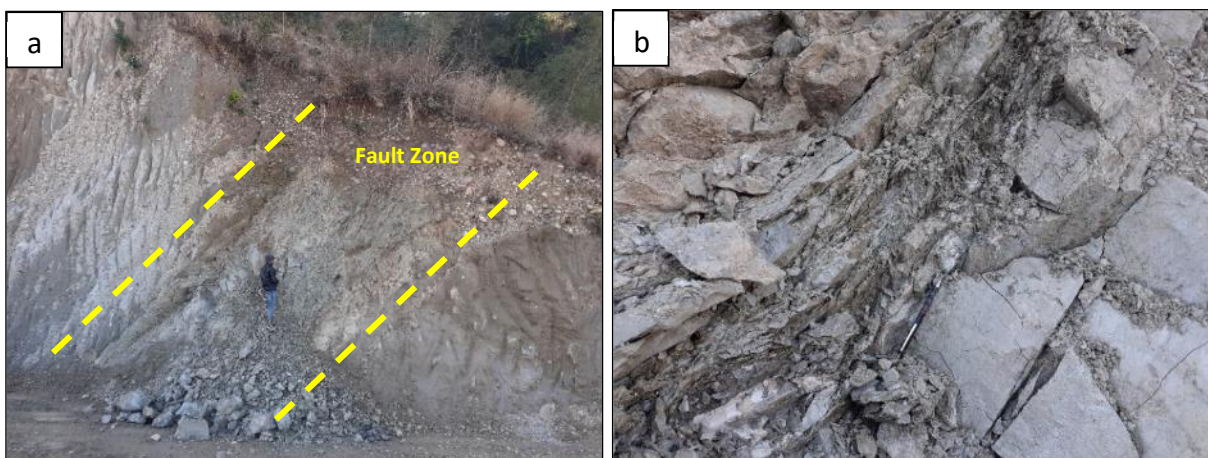


Figure 4.6 (a) Reverse fault with fault plane dipping SW near Sukhar Khad (b) Fault zone in mudstone. Camera facing in NW direction

(Figure 4.4) and towards the eastern side, near Sukhar Khad, the beds have a nearly NW-SE strike and a dip of above 50° southwestwards increasing upto 65° near a southwest dipping reverse fault (Figure 4.6a) of same strike. To the east of this fault, along the Kunnah Khad section, the beds become steeper with dips of about 80° southwestwards to almost subvertical dips.

About 20 xbg activity was recorded in the grey sandstones ~200-400 ppm measured by RSM in this area. The activity is also associated with calcitic cemented lenses, mud clasts, carbonaceous matter.

4.2.3.2 Loharkar

The grey sandstone, pebbly sandstone and pebble beds exposed along Dadh Khad and Kunnah Khad are continuous into the Loharkar area (Figure 4.7). Besides this, coarse grained brown sandstone and medium grained light grey sandstone are also present at places. The sandstone is composed of subangular grains of quartz, feldspar, garnet, some opaques and pyrite. Calcitic cemented lenses, mud lenses and stringers of carbonaceous matter are also found within the grey sandstone. Earlier studies in this area have reported pitchblende, coffinite, tyuyamunite and uranophane as the dominant uranium minerals (Kaul et al., 1993). Radioactivity of about 3-5xbg was recorded in the sandstone.



Figure 4.7 Grey sandstones and pebble beds along stream section along Dadh Khad, near Loharkar

4.2.3.3 Nalti

Grey sandstone with slightly brownish tint and pebble beds dominate the area. Sandstone is medium to coarse grained and

often pebbly, with pebbles arranged along foresets of cross stratifications, which are generally planar or trough type. Pebble beds also show cross stratifications and imbrications. Beds strike NNW-SSE with dips varying from 35° to 60° eastwards (Figure 4.8).



Figure 4.8 Pebble beds with grey sandstone lenses along stream section, near Nalti

Activity of about 6-10xbg was recorded in Nalti and about 15-35xbg in adjoining Har village. The activity is associated with the grey sandstones and the matrix component of pebble beds. Activity of 480ppm was found associated with stringers of carbonaceous matter in Har.

4.2.4 Romehra

The Romehra area, to the southwest of Paniali, along Barsar thrust was also visited during the course of the field work. The rock types in this area are dark grey to dark brown to red coloured mudstone to fine grained sandstone. Mudstones are characterised by earthy fracture and contain very fine clasts of quartz and feldspar which are subrounded to angular. Secondary copper mineralisation is also observed along with uranium mineralisation (Figure 4.9). The activity varies from 4xbg to 50xbg. Earlier studies reported uraninite, autunite and torbenite. The beds strike NW-SE and dips 25-70° southwestwards.



Figure 4.9 Secondary copper minerals associated with uranium mineralisation in Romehra

4.3 Structures

4.3.1 Remote sensing studies to identify structural features

The satellite imagery- IRS LISS III Imagery and Cartosat DEM were processed as per the methodology adopted and used to extract lineaments. PCI Geomatica software was used for the automatic detection of lineaments from the imagery. Manual identification of lineaments were also carried out.

(i) LISS III Imagery

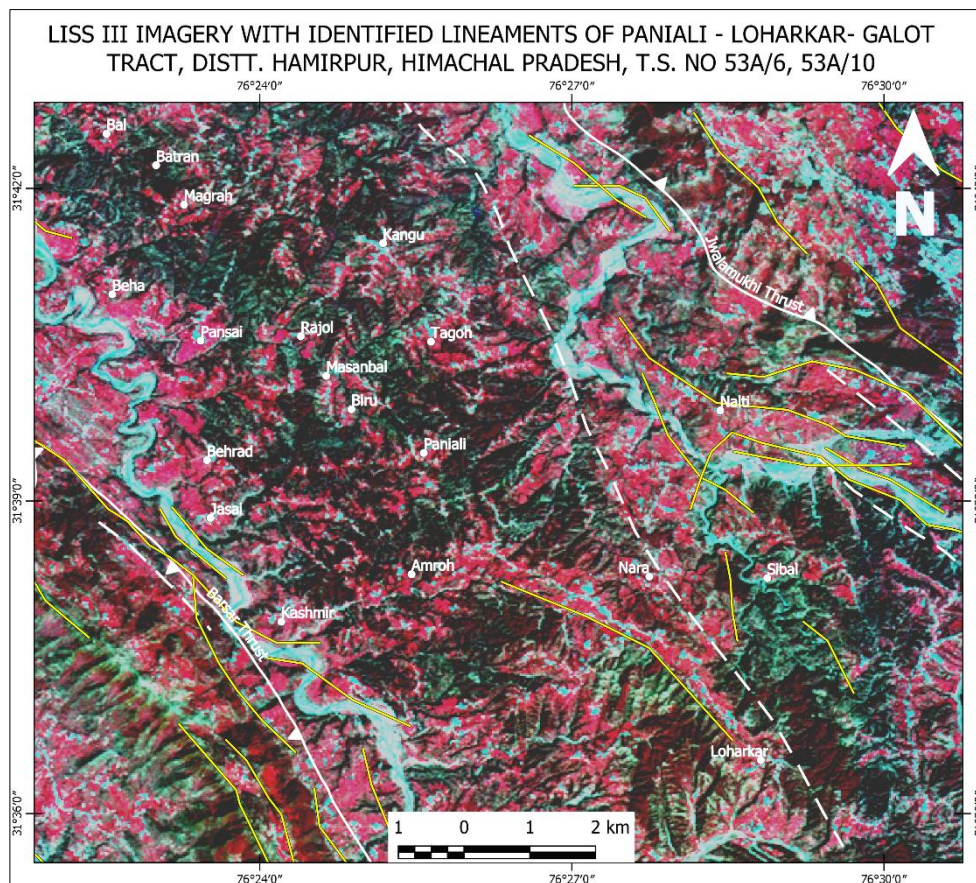


Figure 4.10 Lineament map generated from LISS III Imagery superimposed on FCC composite

Figure 4.10 shows the false color composite (FCC) image based on bands 4, 3 and 2 of LISS III data downloaded from Bhuvan portal of National Remote Sensing Centre (NRSC), pertaining to the study area. Superimposed on the imagery are the identified lineaments. It can be seen that dominant orientations of these lineaments correspond to NW-SE and NE-SW

directions. The NW-SE lineaments have more continuity and length and corresponds to major lineaments in the area, including the Barsar thrust to the west, Jwalamukhi thrust to the east, which are known and available in the published maps..

(ii) Cartosat DEM

The Cartosat based Digital Elevation Model obtained from the Bhuvan portal is shown in Figure 4.11. A shaded relief map prepared from the DEM gives an areal view of the topography with differential shading according to elevation and illumination direction selected. The major lineaments and escarpments are very pronounced in this imagery.

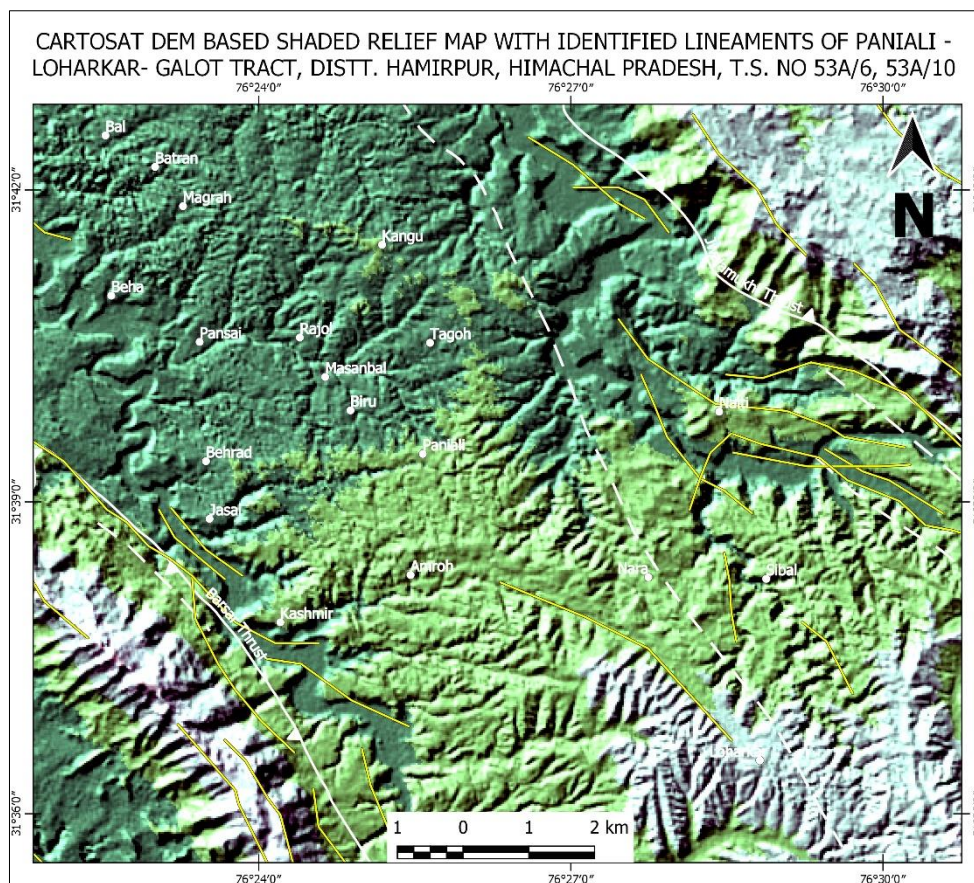


Figure 4.11 Lineament map generated from Cartosat DEM superimposed on Shaded Relief Map

The slope image derived from the DEM using GRASS Tools plugin available with QGIS is shown in Figure 4.12. This image also highlights the major lineaments and the sharp variations in topography. The brightness of the pixels indicate the steepness.

In addition to lineament studies, DEM was also used in obtaining the elevations of field points, along with GPS and toposheet based elevations. Topographic profiles of the area were also prepared using the DEM for understanding the variations in lithology.

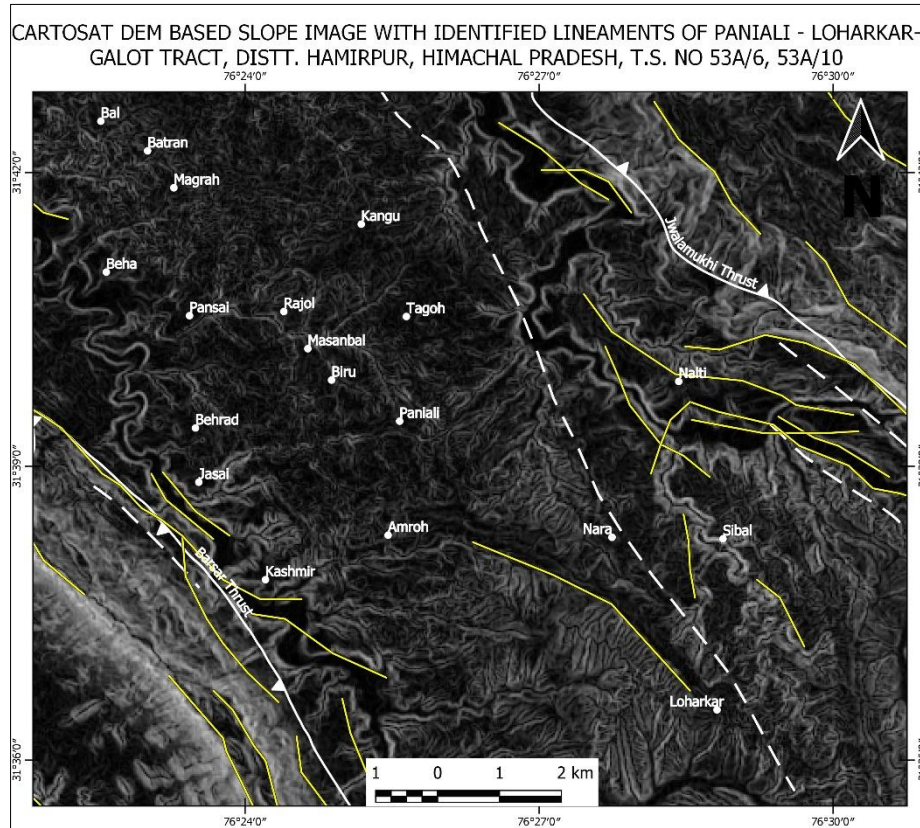


Figure 4.12 Lineament map generated from Cartosat DEM superimposed on Slope image

Field observations

Ground verification of the lineaments were carried out during field work and different geological as well as geomorphological structures were identified. The major NW-SE trending lineaments are the Barsar and Jwalamukhi Thrusts whereas within - basin slips and local scale faults occur at places (Figure 4.13). Steep river bank escarpments and ridges with dip slopes (Allaby, 2013) represent the common geomorphic lineaments (Figure 4.13).

The attitude of the sediment bedding planes show general NW-SE strike and dip amounts varying from horizontal and sub horizontal to subvertical, with beds dipping in both NE and SW directions. Two synclinal structures are observed to be associated with both the

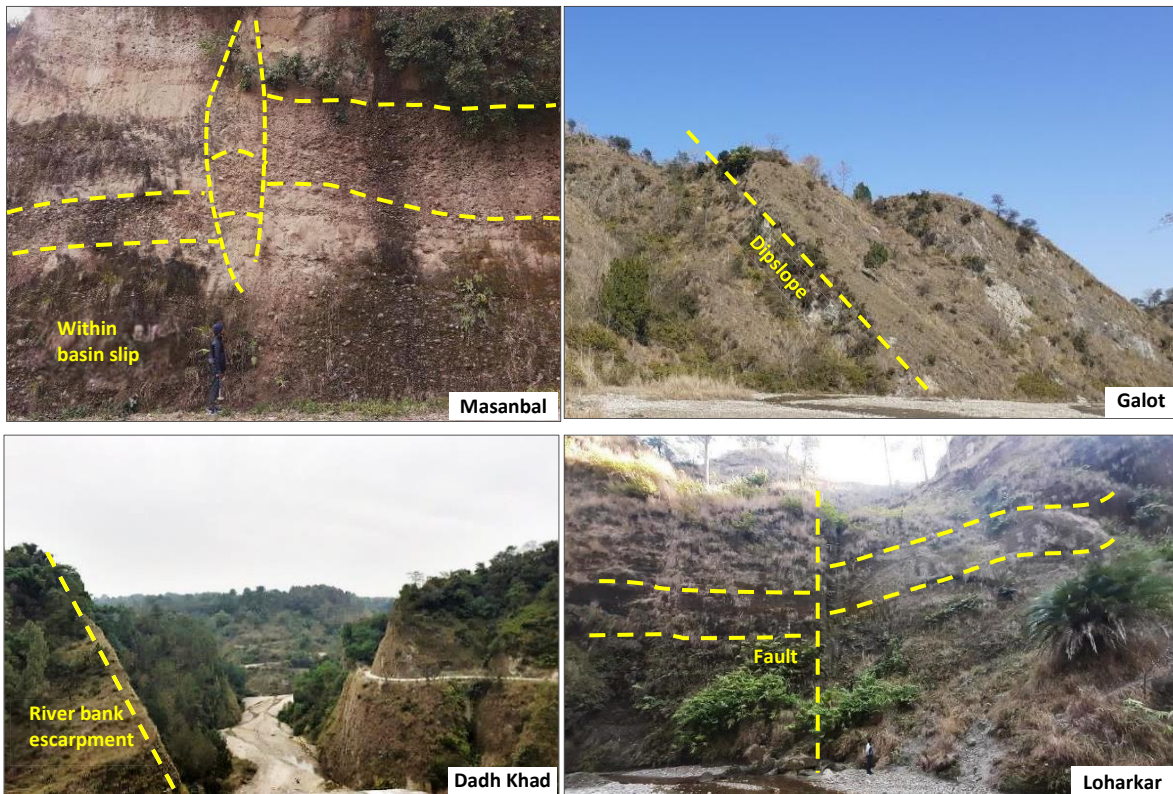


Figure 4.13 Lineaments in the study area identified during field work and ground verification.

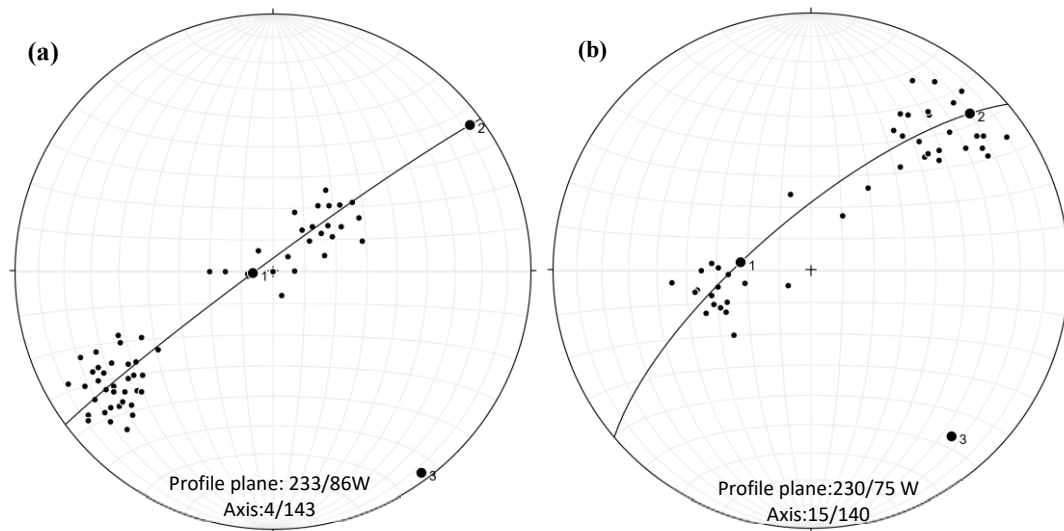


Figure 4.14 Lower hemisphere equal area projections of bedding plane orientations from synclinal structures associated with (a) Barsar Thrust (b) Jwalamukhi Thrust

Jwalamukhi and Barsar Thrusts within the study area. To the west of Jwalamukhi Thrust, the Middle Siwalik forms the Bakarti syncline (Kaul et al., 1993) whereas the Upper and Middle Siwalik to the east of Barsar thrust form the Balaru syncline. The attitudes of beds collected from both synclinal structures were plotted on lower hemisphere equal area projections as poles

to the bedding planes (Figure 4.14). By fitting great circles to the clusters of poles, the profile planes and fold axes were determined. Both folds have NW-SE trending fold axes, parallel to the thrusts. Whereas the fold axis of the Balaru syncline is sub horizontal, the Bakarti syncline has a gentle plunge of 15° southwestwards.

4.3.2 Geological map of the area

The geological map of the Paniali-Loharkar-Galot tract (1:25000 scale) and the surroundings is shown in Figure 4.15. This map was prepared in QGIS 3.8.3 Zanzibar software. The geological map has been superimposed on the DEM. Structural data and radioactive anomalies are also plotted.

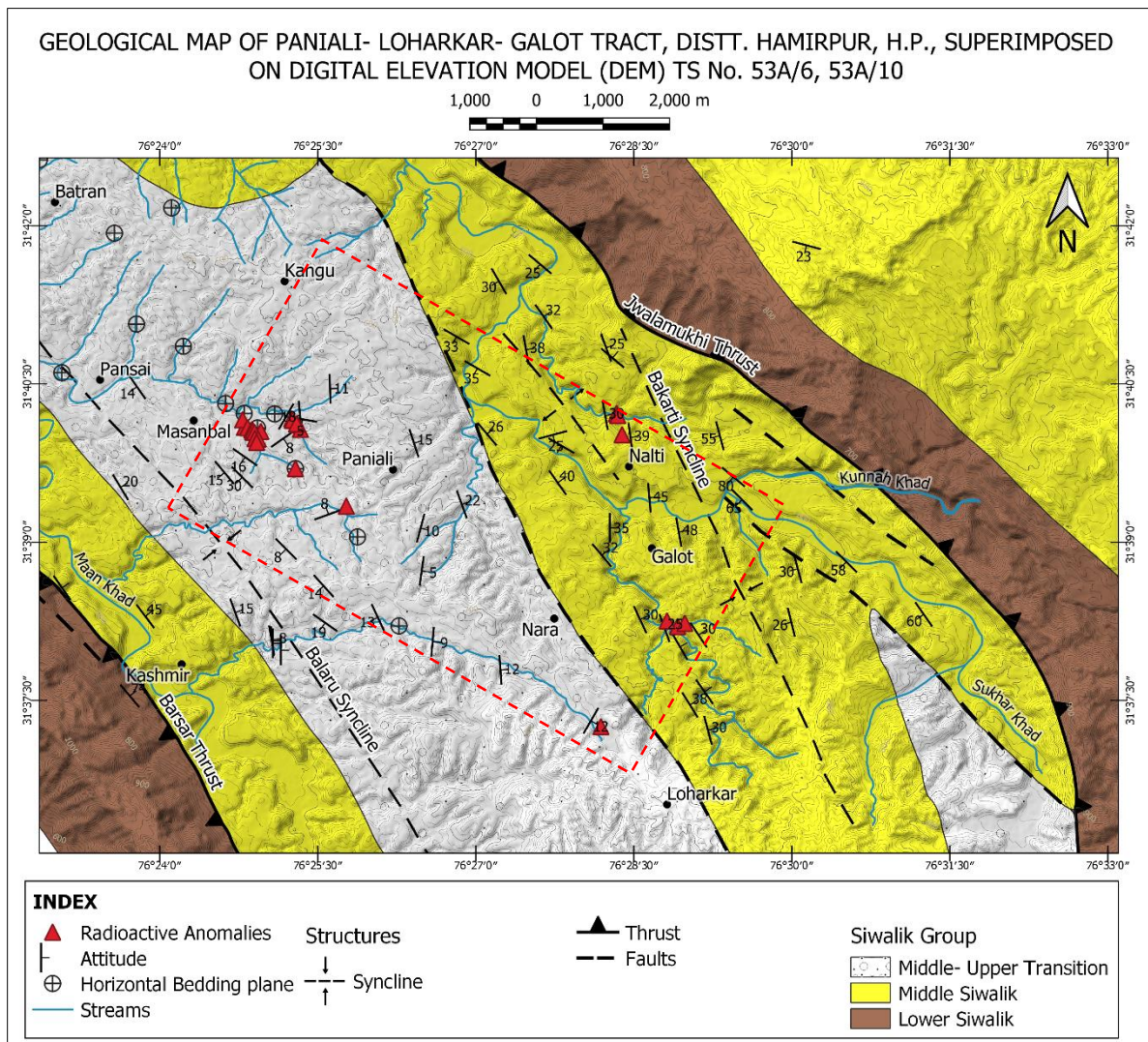


Figure 4.15 Geological Map of the study area, superimposed on the Digital Elevation Model

CHAPTER 5

RESULTS AND INTERPRETATION

5.1 Radiometric Studies

The collected grab samples were radiometrically assayed using Beta-gamma and gamma ray spectrometric analyses. The radioactive samples assayed with U_3O_8 values ranging from 0.012 % to 0.071 % (n=10). Samples from Loharkar Galot area assayed with U_3O_8 values range from less than 0.01 % - 0.28 % (n=7). Physical assay results of the radioactive samples are given in Table 5.1.

Table 5.1 Table showing the physical assay results of radioactive samples from Masanbal and Nalti area, Dist. Hamirpur, H.P.

Table : Radiometric assay results of samples from Paniali-Loharkar-Galot tract, dist. Hamirpur, H.P.				
Area	Sample No.	e U_3O_8 %	U_3O_8 %	Ra(e U_3O_8) %
Masanbal- Biru- Paniali	RA-18	0.036	0.071	0.028
	RA-19	0.028	0.027	0.021
	RA-20	0.028	0.054	0.021
	RA-21	0.031	0.029	0.025
	RA-22	0.022	0.042	0.016
	RA-23	0.049	0.017	0.044
	SI/RA/3	0.010	0.012	0.009
	SI/RA/14	0.011	0.019	0.010
	SI/RA/4	0.014	0.022	0.013
Loharkar- Galot- Nalti	SI/RA/6	0.026	0.067	0.025
	SI/RA-1	0.020	0.088	0.019
	SI/RA-2	0.085	0.280	0.085
	SI/RA-3	0.011	<0.010	0.010
	SI/RA-4	0.077	0.057	0.076
	SI/RA-5	0.014	<0.010	0.013
	SI/RA-6	0.050	0.097	0.049
	SI/RA-7	0.350	0.020	0.340

5.2 Petrographic studies

Petrographic studies reveal that the sandstones are clast supported with upto 3 - 6 % of matrix and upto 6 % cement, which is dominantly calcitic with occasional ferruginous cement. The framework is composed of subangular to subrounded clasts, dominantly of quartz (40 – 60 %), feldspar (10 – 25 %) - both plagioclase (45%) and K-feldspar (55 %), rock-fragments (14–30 %) and mica (3 – 4 %). The rock fragments dominantly comprise of sedimentary/metasedimentary

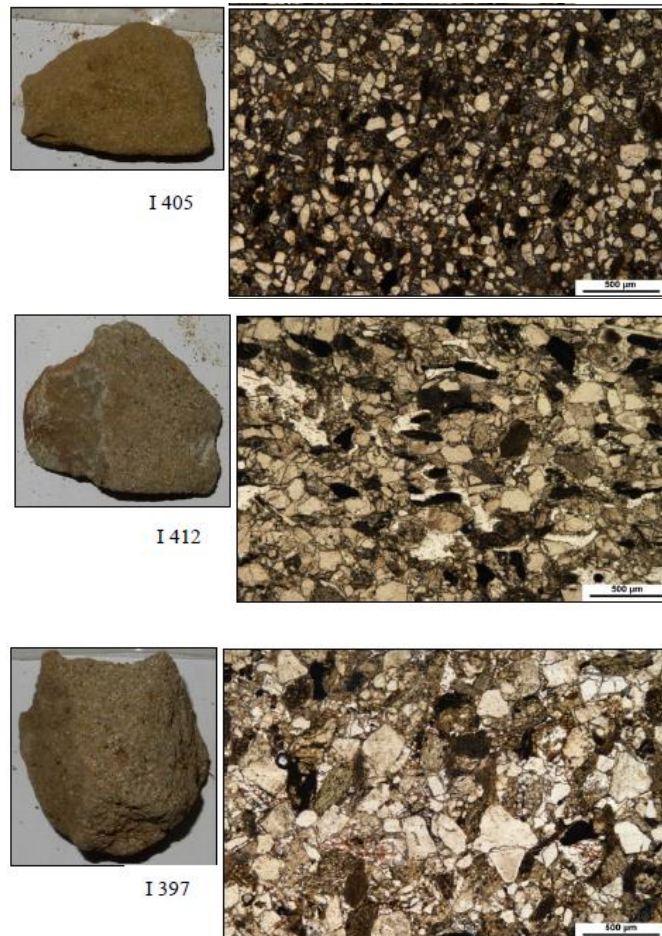


Figure 5.1 Few selected photomicrographs (PPL) of noradioactive samples from the study area

clasts (87 %) - shale.siltstone, sandstone, chert and mudstone, metamorphic clasts (12 %) - metaquartzite, phyllite, schist and clasts of igneous rocks-mainly granitoids (18 %). Variations are observed in grain size, shape and sorting across different units. Alteration of feldspar and formation of pseudomatrix also has been reported. Photomicrographs of few selected sandstone samples of different grain sizes are shown in Figure 5.1. The study results suggest a general nomenclature of the sandstone units as sublithic to feldspathic lith-arenite.

The sandstone from Masanbal area is medium to coarse grained, ill sorted, consisting of subrounded to subangular grains of dominantly quartz (~25 - 58 %), feldspar (5 – 7 %), lithic fragments-dolerite, polycrystalline quartz, granite mylonite (~35 – 67 %), mica (muscovite and

biotite). The matrix components are clay, calcite and carbonaceous matter. Occasionally, floating calcite grains are also observed within the matrix (Figure 5.2). The cement is dominantly calcitic with occasional ferruginous cement. Framboidal pyrites are found to be associated with carbonaceous matter and give α -tracks in CN films (Figure 5.2 and 5.3). Feldspar has commonly altered to sericite whereas pyroxenes clasts have altered to chlorite (Figure 5.2).

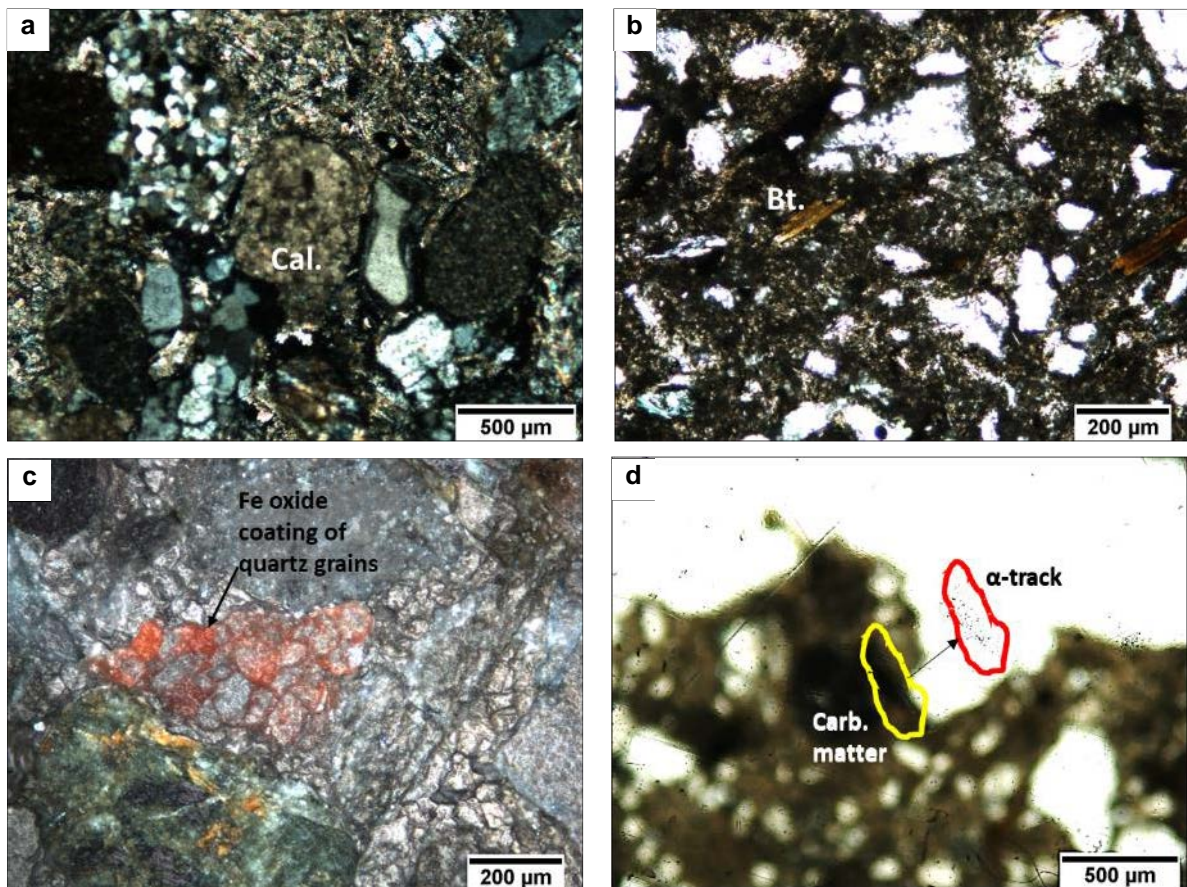


Figure 5.2 (a) Calcite (sparry) in lithic arenites (b) Matrix with clay and carbonaceous matter. Feldspar disintegration along grain boundary (c) Fe-oxide coating of quartz grains revealed in reflected light (d) carbonaceous matter in the matrix along with corresponding α -track.

α -tracks are observed to be associated with the matrix portion of the sandstone composed of clay and carbonaceous matter in CN film studies (Figure 5.3). 50/100x oil

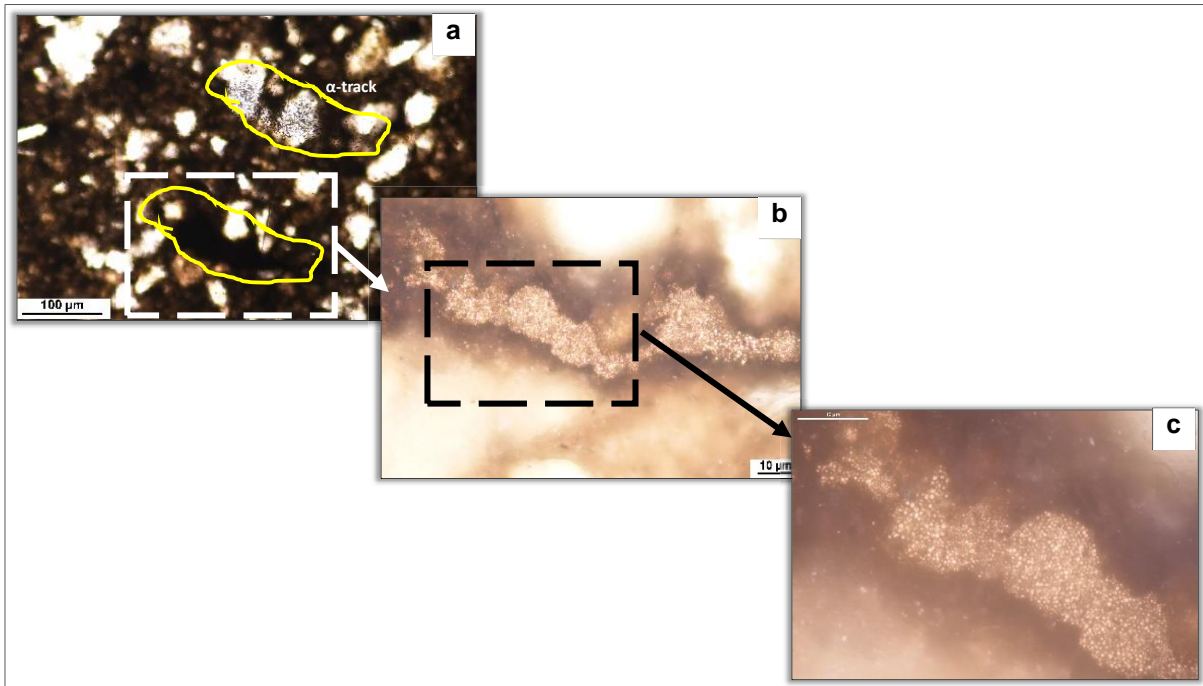


Figure 5.3 (a) Matrix with clay and carbonaceous matter with corresponding α -track. (b) and (c) Framboidal pyrite seen at higher magnification in oil immersion. The outer rim shows evidence of oxidation.

immersion studies (in reflected light) revealed that framboidal pyrite is also associated with carbonaceous matter. Fine white grey specs (colloform) appears to be radioactive. Most of the framboidal pyrite bundles associated with radioactivity are partially oxidised along their rim, which is suggestive of Fe- oxidation and U- reduction.

Samples from Paniali area contain more ferruginous cement in the matrix and less clay. Hematite is occasionally present and the clasts are iron oxide coated. Framboidal pyrite is also observed.

5.3 XRF Analysis

The X-ray Fluorescence analysis of samples (n=30) carried out at WDXRF laboratory, AMD Nagpur revealed the major and trace element composition of the sandstones. These samples are characterised with variable SiO_2 (62.15 – 74.80 %), Al_2O_3 (11.38 – 16.02 %), Fe_2O_3 (3.53 – 13.93 %), MgO (1.40 – 4.19 %), CaO (0.44 – 5.25 %), Na_2O (1.80 – 2.56 %) and K_2O (2.16 – 3.75 %) content. The trace element data shows varying content of Cr (143 - 510 ppm),

Rb (80 - 174 ppm), Zr (64 - 148 ppm), Ba (520 - 890 ppm), Ce (102- 232 ppm), Th (13 - 42 ppm) and U (824 - 2549 ppm).

The major oxide data are used for generating various plots for geochemical classification as well as to decipher the tectonic environment at sediment source (Bhatia,1983). Variation between oxides were plotted on to Harker diagrams.

The plot of $\log (\text{Na}_2\text{O} / \text{K}_2\text{O})$ vs $\log (\text{SiO}_2 / \text{Al}_2\text{O}_3)$ after Pettijohn et al. (1987), for geochemical classification of sandstones is shown in Figure 5.4. The samples from Galot-Loharkar area fall in the field of litharenites while the samples from Masanbal - Paniali area fall in the field of graywacke. This also correlates with field and petrographic observations that the matrix content in Masanbal-Paniali samples are relatively higher compared to that of Galot-Loharkar.

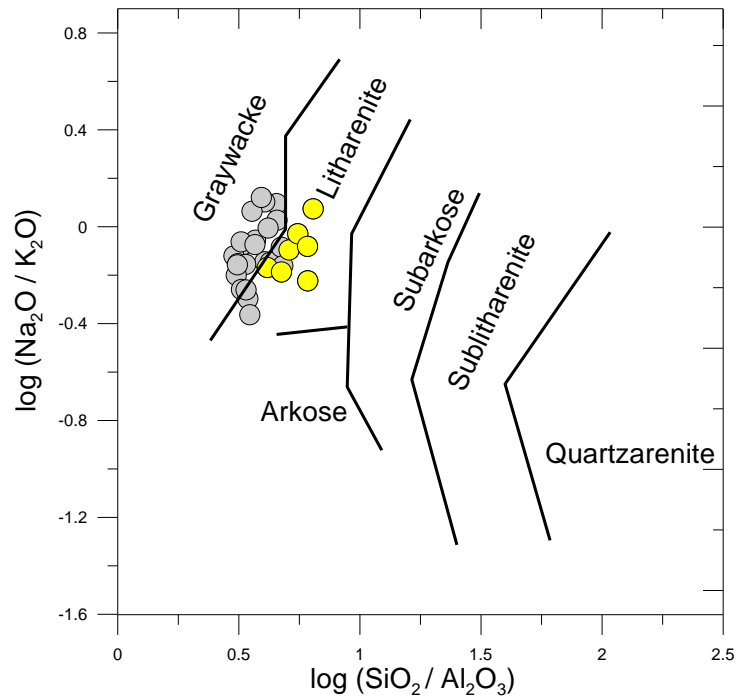


Figure 5.4 Plot of $\log (\text{Na}_2\text{O} / \text{K}_2\text{O})$ vs $\log (\text{SiO}_2 / \text{Al}_2\text{O}_3)$ after Pettijohn et al., (1987) for geochemical classification of sandstones.

The TiO_2 vs Al_2O_3 plot of Amajor (1987) is shown in Figure 5.5. The lower the TiO_2 - Al_2O_3 ratio, more depleted is the source rock in Ti bearing minerals. The TiO_2 vs Al_2O_3 plot of the studied samples show that these samples fall in the field of granite to granite basalt provenance, indicative of a mixed provenance of these samples.

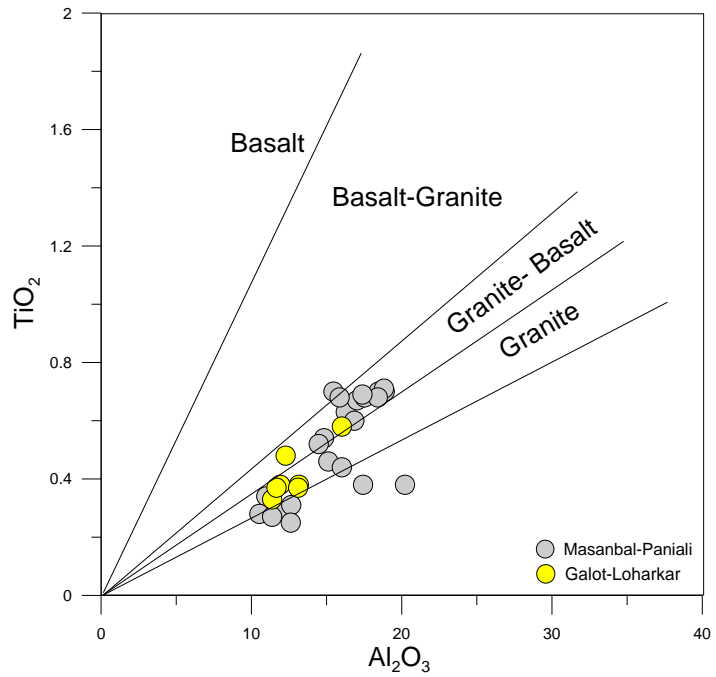


Figure 5.5 TiO_2 vs Al_2O_3 plot for discriminating the source rock characteristics

The provenance tectonic setting can be inferred from the major oxide compositions (Krooneneberg, 1994; Maynard et al., 1982; Roser and Korsch, 1986). The plots of major oxide ratios can be used to discriminate four major tectonic provinces namely oceanic island arc, continental arc, passive margin and active continental margin. The samples from this study plot across the passive margin and active continental margin fields of the Na_2O/K_2O vs SiO_2 diagram (Figure 5.6) of

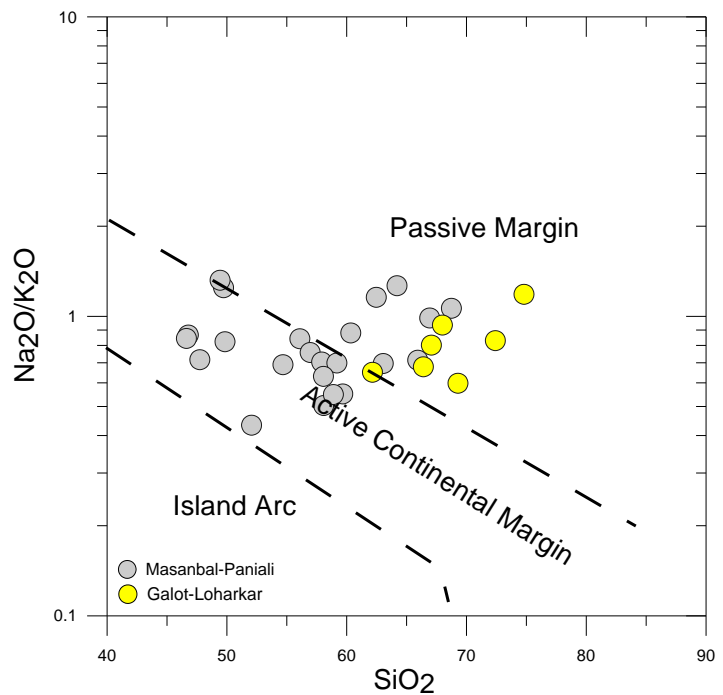


Figure 5.6 Na_2O/K_2O vs SiO_2 diagram of Roser and Korsch (1986).

Roser and Korsch (1986). The samples from Galot - Loharkar area dominantly fall in the passive margin field while those from Masanbal - Paniali area fall dominantly in the active continental margin field. Few samples of the latter set also fall in the passive margin field as well as along the boundary of both the fields.

In the $\text{SiO}_2 / \text{Al}_2\text{O}_3$ vs $\text{K}_2\text{O} / \text{Na}_2\text{O}$ diagram (Figure 5.7a) of Maynard et al. (1982) also the samples plot across the passive and active margin fields with Galot-Loharkar samples and Masanbal-Paniali samples dominating the passive margin field and active continental margin field respectively. Figure 5.7b shows the ternary plot of $\text{SiO}_2 / 20 - (\text{Na}_2\text{O} + \text{K}_2\text{O}) - (\text{TiO}_2 + \text{Fe}_2\text{O}_3 + \text{MgO})$ (after Kroonenberg, 1994). In this plot as well, most samples fall in the passive margin field, along the zone with overlap of continental island arc setting.

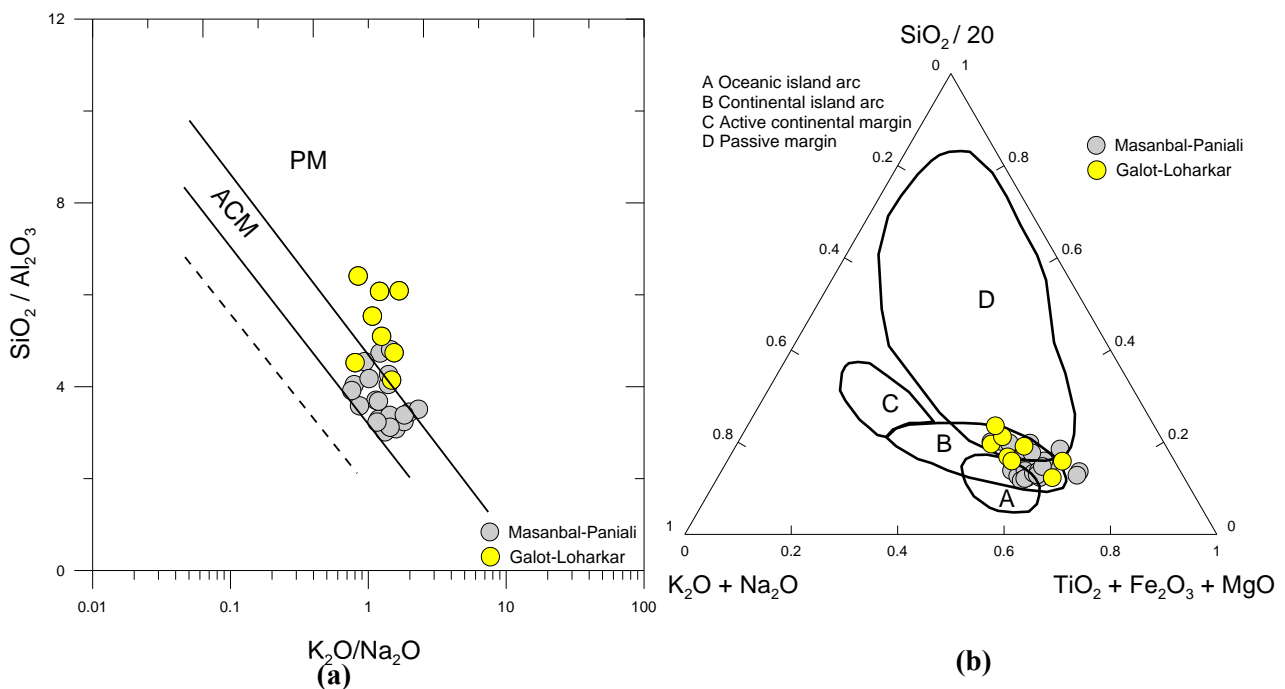


Figure 5.7 (a) $\text{SiO}_2 / \text{Al}_2\text{O}_3$ vs $\text{K}_2\text{O} / \text{Na}_2\text{O}$ diagram of Maynard et al. (1982) *PM* Passive Margin, *ACM* Active Continental Margin (b) ternary plot of $\text{SiO}_2 / 20 - (\text{Na}_2\text{O} + \text{K}_2\text{O}) - (\text{TiO}_2 + \text{Fe}_2\text{O}_3 + \text{MgO})$ (after Kroonenberg, 1994). *A* Oceanic island arc, *B* continental island arc, *C* active continental margin, *D* passive margin

5.4 Carbon and Sulphur Analysis

A few selected samples (n=9) from the study area were analysed for their carbon and sulphur content. Table 5.2 shows the data of sulphur %, total organic carbon (TOC %), total inorganic carbon (TIC %). The total organic carbon % varies from 0.14 % to 0.33 %, which corroborates with the petrographic observation of presence of carbonaceous matter in the matrix of sandstone. The total inorganic carbon (TIC %) varies from 0.48 % to 2.42 %, which is due to the presence of calcite cement.

Table : Carbon and Sulphur Analysis results of samples from Paniali-Loharkar-Galot tract				
Sl. No.	Sample No	S %	Total Organic Carbon (TOC) %	Total Inorganic Carbon (TIC) %
1	SI/SNK/AV/RSA/RA-6	<0.10	0.33	0.86
2	SI/SNK/AV/RSA/RA-14	0.36	0.48	2.13
3	SI/SNK/AV/RSA/RA-19	<0.10	0.37	<0.10
4	SI/SNK/AV/RSA/RA-22	<0.10	0.34	<0.10
5	SI/SNK/AV/RSA/RA-23	<0.10	0.43	0.48
6	SI/SNK/AV/RSA/RA-8	<0.10	0.14	<0.10
7	SI/SNK/AV/RSA/RA-10	<0.10	<0.10	2.42
8	SI/SNK/AV/RSA/RA-12	<0.10	<0.10	<0.10
9	SI/SNK/AV/RSA/RA-13	<0.10	<0.10	<0.10

Table 5.2 Table showing the results of carbon and sulphur analysis of samples from Paniali-Loharkar-Galot tract, Dist. Hamirpur, H.P.

CHAPTER 6

DISCUSSION

6.1 Field observations

An attempt has been made to prepare a 3D visualisation of the field data and anomalies, along with the structural pattern of the study area- Paniali-Loharkar-Galot tract and its adjoining parts (Figure 6.1). An interactive 3D plot was prepared for the field data with GPS generated coordinates of Latitude, Longitude and Elevation, in a Python based programming environment. A suitable viewing angle was determined from this interactive 3D plot for 2D projection, so as to contain maximum information and to carry out further additions. A 3D block diagram was constructed based on the projection generated from Python, in Corel Draw. The regional geological map was projected on to the top surface, schematic structural profile based on collected and available structural data was projected to the sides and the radioactive anomalies were also projected on to their respective locations on the map at the top. Actual topographic profile along the faces of the block were extracted from the Cartosat based Digital Elevation Model (DEM) using QGIS and are projected along the sides. It has to be noted that the north direction in the diagram points differently from the convention used in maps. This is made for the convenience, so as to facilitate proper projections of individual features in the diagram, with best details. Lateral variation in lithology and certain other details were omitted in order to avoid cluttering.

The block diagram depicts the actual positions of the surface anomalies in the three dimensional space. The study area is bounded by Jwalamukhi Thrust (not shown in the block) to the east and Barsar Thrust to the west. A faulted contact between the Middle and Upper Siwalik Group divide the area into an eastern and western block. Simplified lithological sections for each block is given along the left rear (SE) and front right (NW) corners

respectively. In the eastern block, thick succession of grey, medium to coarse grained sandstone with pebble bed lenses dominate the lithology. To the southeastern part, along Dadh Khad and Loharkar, grey coarse grained sandstones host mineralisation, at relatively higher elevations than Nalti and Masanbal. Nalti area falls along the axial part of a regional synclinal structure to the north of Dadh Khad and activity in grey sandstones as well as in the matrix component of pebble beds which dominate the lithology of the area. Along Masanbal, grey, coarse sandstone with calcitic cemented lenses, mud clasts and carbonaceous matter host discontinuous patchy activity, which is mapped in the present study. This is at much lower elevation and is overlain by thick succession of oxidised medium to fine grained sandstone with pebble horizons, show lateral variation in colour on the map and variation along vertical section. Transition of buff, limonitic yellow, brown and greyish brown colorations are observed vertically downwards in the sediments, indicative of increasing reducing conditions downwards. The radioactive anomaly in this area is also found to increase with depth. To the north of Masanbal, the activity dies down to background and further north where two streams meet, abrupt increase in the clast size of pebble beds and decrease in the proportion of sandstone is observed, along with lateral displacement of strata along E-W direction. Even further north, fine greenish grey sandstone with mud clasts are observed, along Pansai.

6.2 Structures

The synclinal structures associated with both thrusts enclosing the study area are asymmetric with their steeper limb towards the thrust, which suggests that they may have formed as footwall synclines associated with fault propagation folding. Such type of folds are associated with detachment faults without involving basement rocks (McNaught and Mitra, 1992), like the Barsar and Jwalamukhi Thrusts. Further, seismic studies in the Kangra sub basin also indicate that the Barsar Thrust is a shallow thrust and is linked to a detachment fault at its base, along the lower part of the basin. It is possible that this fault system facilitated the

circulation of fluids between deeper part of the basin and the surface, which is substantiated by the presence of copper mineralisation at Romhera, in the Lower Siwalik mudstones along Barsar Thrust. Magnetotelluric studies have also suggested the presence of good conductors at depth within the Siwalik sediments (Veeraswamy et al., 2010).

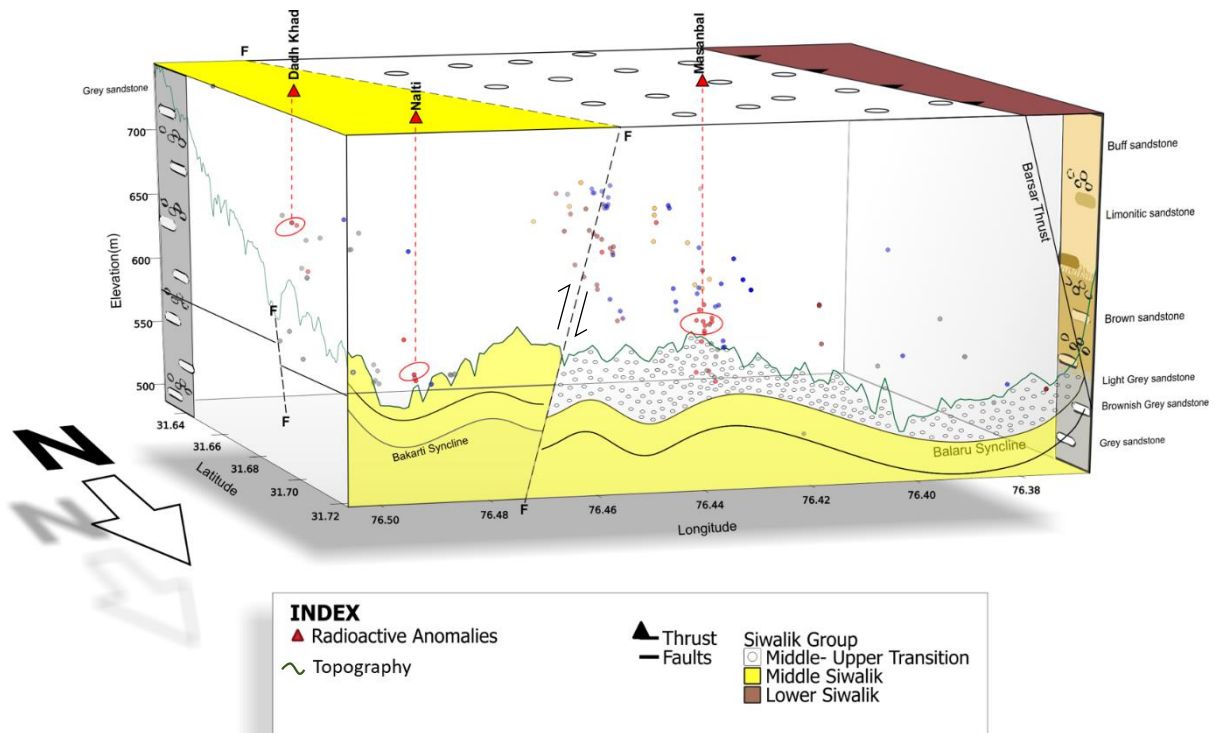


Figure 6.1 A representative 3D block diagram based on interactive plot generated from GPS based field data along with geological and structural information. The dots represent data points in the 3D space, with red dots corresponding to surface anomalies. Orientation of the block with respect to north direction was decided based on the suitable viewing angle generated from the interactive plot.

6.3 Oxidation of sediments and faulting

Oxidising fluids invading the sandstones from near surface conditions resulted in the oxidation of Fe bearing minerals to oxides and hydroxides. Bandings of iron hydroxides and oxidation haoles around mud clasts formed within these sediments. Later faulting along the NW-SE trending fault plane, has uplifted the eastern block, exposing the relatively less oxidised grey sandstones, which are exposed at elevations of about 900 m. In the western part of the area, the oxidised sandstone with vertical colour variations consists of the top 100-150m

of exposed stratigraphy, at elevations below 650m and the grey sandstone, with radioactivity appears only at 500 – 540 m elevation. The presence of oxidation haloes and iron oxide coated pebbles with corona structures indicate the prevalence of oxidation phenomena in these sandstones. Similar sandstones are observed towards the hinge part of the Bakarti syncline as well. It may be inferred that faulting is later to the oxidation of sediments. Cross faults of strike slip nature cut across the regional strike of the faults and synclinal structures. Minor slip faults have also developed in association with these faults at places.

6.4 Intensity of oxidation and radioactivity

It has been observed that while the colour of the rock changes from buff to brown to grey with stratigraphic depth, the mud clasts in these sandstones, also change in nature. In the

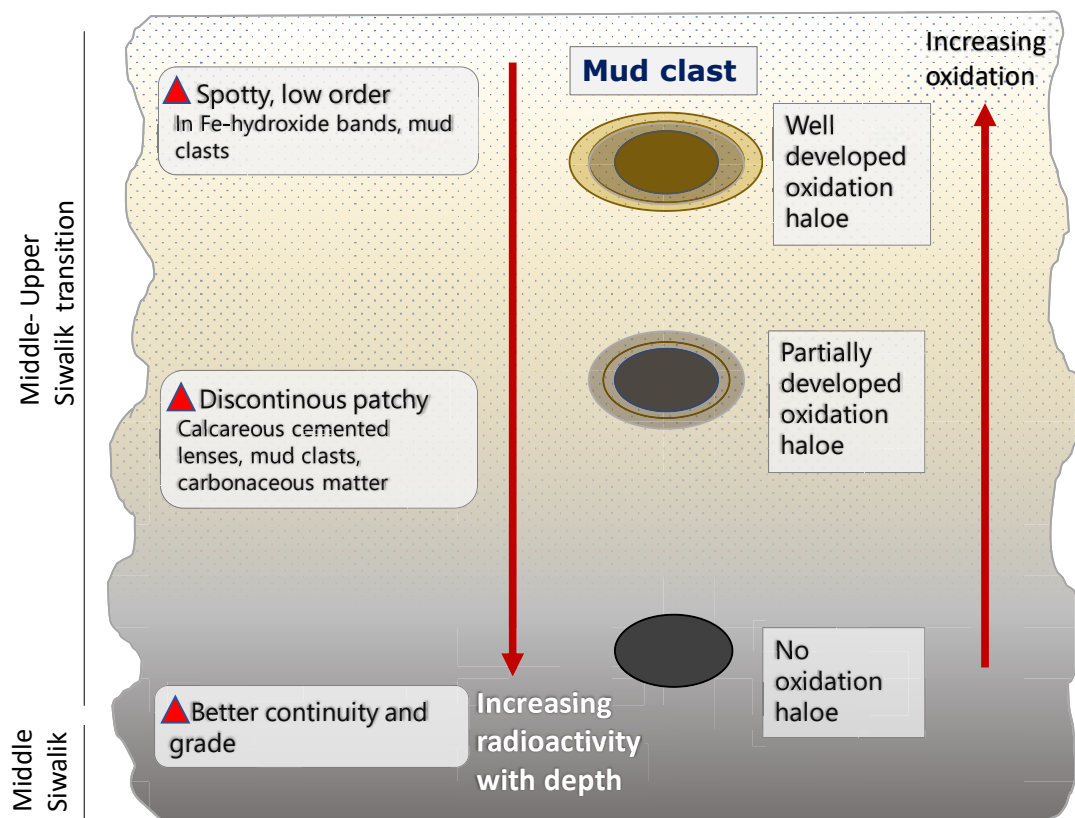


Figure 6.2 Representative diagram showing the variation in the redox condition of mud clasts, sandstones and radioactivity with increasing depth.

top most units, mud clasts have well developed oxidation haloes whereas the core of the clasts appear brownish. To the bottom, the haloes gradually reduce and disappear while the core

changes from brown to light grey to dark grey (Figure 6.2). This variation suggests changes in redox conditions with depth. It is to be noted that the increase in radioactivity with depth also can be correlated with this change. The activity occurs as spotty and of low order nature near the surface in the buff sandstones and is associated with the mud clasts and iron oxide bands whereas with depth, it becomes patchy with improved extend and occurs in mud clasts, sandstone and with carbonaceous matter.

6.5 Petrography

The clast composition comprising quartz and feldspar clasts, lithic fragments of sedimentary, metamorphic and igneous origin indicate sediments were derived from felsic plutonic and metamorphic rocks, and reworked earlier sediments. A subordinate source of volcanic suites is also recognised from the presence of volcanic clasts. Therefore, a mixing of source rocks is suggested by the clast mineralogy.

Autoradiography study using CN films suggest that the radioactivity is associated with carbonaceous matter as well as clay in the matrix component of the sandstone. This is indicative of U being present mostly in adsorbed form. The presence of oxidation rims around framboidal pyrite suggests that reduced U may be present at places where activity occur in the vicinity of framboidal pyrites.

6.6 Geochemical characterisation

Geochemical data suggests that the sandstone samples from Galot -Loharkar area and Masanbal-Paniali area show slightly distinct characteristics. The sediment source of these rocks as indicated by the TiO_2 vs Al_2O_3 plot of Amajor (1987) is dominantly granite- granite basalt, suggestive of mixed source. The presence of lithic fragments of varying rock types observed in petrographic study correlates well with this observation. The geochemical classification diagram of discriminates samples from Galot-Loharkar area as litharenites and those from

Masanbal-Paniali area as graywackes. This may be attributed to the relatively higher amount of clayey material present in the matrix of the Masanbal- Paniali sandstone samples. The source tectonics as revealed from the major oxide plots suggest a transition from passive margin to active continental margin tectonic regime. The Galot-Loharkar sandstones were sourced from a passive margin tectonic setting while the Masanbal-Paniali sandstones range from passive to active margin but dominantly show active continental margin signature. This observation is well in accordance with the findings from similar works carried out in Siwalik by Kundu et al (2016), Sinha et al. (2007) and Ranjan and Banerjee (2009).

The low total organic carbon content (TOC < 0.5%) and very low sulphur (< 0.10) in the studied samples indicate insufficient precipitation of pyrite which is required to provide reducing conditions for uranium mineralisation.

6.7 Geology, tectonic setting and mineralisation

The transition from Middle Siwalik to Upper Siwalik occurred in consequence with onset of tectonic activity along the Main Boundary Thrust (MBT) around 5 Ma (Kumar et al., 2013). The transition from distal to proximal sedimentation near the active thrust front resulted in the variations observed in the sediment characteristics. The sandstones of Masanbal-Paniali area stratigraphically overlay those of Galot -Loharkar area and are characterised by the sediments in the transition zone between the Middle and Upper Siwalik represented by a sandstone dominated lower part and pebble bed dominated upper part. Geochemical classification and tectonic discrimination diagram also suggest that the geology of this zone marks the transition from a passive margin to active continental margin tectonic setting of the sediment source. The sediments were derived from multiple suites of rocks, as indicated by petrographic and geochemical data. Decreasing intensity of oxidation and increasing intensity of radioactivity are observed with stratigraphic depth in this zone. The adsorbed nature of

radioactivity observed in petrographic studies indicate that the uranium in remobilised form was adsorbed by the carbonaceous matter and clay in the matrix of the sandstones. Given the abundance of clay and disseminated carbonaceous matter in the Middle and Upper Siwalik sequences, the restricted occurrence of radioactivity along the transition zone may have been controlled by remobilisation of uranium associated with the tectonic activity along MBT.

CHAPTER 7

CONCLUSION

The present study integrating remote sensing, field mapping and laboratory studies has delineated the lithostructural characteristics of the Middle Siwalik and Middle-Upper Siwalik transition sediments in the Paniali-Loharkar-Galot tract of Kangra sub-basin. The structural architecture, the transitional sedimentary sequence, changes in provenance tectonic setting, variations in radioactivity and oxidation with depth are revealed.

The sedimentary sequence in the area gradually transitions from grey sandstone of Middle Siwalik to overlying brown to buff sandstones and eventually into pebble beds of Upper Siwalik. These sediments were sourced from multiple provenance, with tectonic setting changing from passive margin to active continental margin. Uranium in the transition zone sediments occurs mainly in adsorbed form with clay and organic matter in the matrix of grey sandstone, while associated with oxidised framboidal pyrites at places. Organic carbon and sulphur content in studied samples are in insufficient concentrations for forming typical sandstone type uranium deposit. But the variation in the intensity of oxidation and radioactivity with depth in this zone indicates horizons with better continuity and grade of mineralisation may be concealed below. The transition of the sediment characteristics and inferred source tectonic settings may be related to the reactivation of Main Boundary Thrust around 5 Ma. Continued fault propagation in the Himalayan foreland basin resulted in thrusting, faulting and folding which are manifested majorly as NW-SE trending lineaments including the Barsar thrust, Jwalamukhi thrust, their associated synclines and NW-SE trending reverse fault. These later events also have spatially displaced the sediments and the uranium mineralized horizons. Hence, it is inferred that the uranium mineralisation in the study area is primarily having a lithological control, while structure has displaced the mineralisation on a later stage.

Insights from the present study has created scope for further detailed studies, which could not be incorporated in this thesis due to timeframe limitations. The presence of clay and mud clasts, variations in their characteristics observed in field, association of uranium in adsorbed form suggest that the clay mineralogy be studied in detail. This can involve separation of clay from the sandstone and analysis using techniques like X-ray Diffraction (XRD) and Scanning Electron Microscopy (SEM). This can be focused on identifying whether any particular clay mineral is playing any role in the adsorption of uranium. Heavy mineral separation and analysis can be adopted for more accurate provenance studies. A focused study to understand the precipitation of calcite to form cemented lenses within the sandstone can also be carried out. Whether this process has relation to invasion of fluids into the basin, uranium mineralisation, and oxidation of sediments can also be studied. Detailed sedimentological studies in a larger area around the present study area can be taken up for facies analysis. The role of neotectonics in the area and its effect on uranium mineralisation also command a detailed study.

REFERENCES

- Allaby, M. (Ed.). (2013). A dictionary of geology and earth sciences. Oxford University Press, p.660.
- Allen, P. A., and Allen, J. R. (2013). Basin analysis: Principles and application to petroleum play assessment. John Wiley & Sons, p.619.
- Alshaghdari, Mohsen. (2017). Geological mapping using open source QGIS. 10.13140/RG.2.2.11978.47045., p.22
- Amajor LC (1987) Major and trace element geochemistry of Albian and Turonian shales from the Southern Benue trough, Nigeria. *J Afr. Earth Sci*, v.6. pp.633–641.
- Baral, S. S., Das, J., Saraf, A. K., Borgohain, S., and Singh, G. (2016). Comparison of Cartosat, ASTER and SRTM DEMs of different terrains. *Asian Journal of Geoinformatics*, v.16(1), pp.1-7
- Bhatia MR (1983) Plate tectonics and geochemical composition of sandstones. *J Geol* 91. pp.611–627.
- Boileau, V. H., and Kohli, G. (1952). Final report on the geology of the Jawalamukhi area. Kangra District, Punjab (1), unpublished report of the Geological Survey of India.
- Brown, R. L., and Nazarchuk, J. H. (1993). Annapurna detachment fault in the Greater Himalaya of central Nepal. *Geological Society, London, Special Publications*, v.74(1), pp. 461-473.
- Crawford, A. R. (1974). The Indus suture line, the Himalaya, Tibet and Gondwanaland. *Geological Magazine*, v.111(5), pp. 369-383.
- Critelli, S., and Ingersoll, R. V. (1994). Sandstone petrology and provenance of the Siwalik Group (northwestern Pakistan and western-southeastern Nepal). *Journal of Sedimentary Research*, v.64(4a), pp.815-823.
- Dahlstrom, C. D. (1970). Structural geology in the eastern margin of the Canadian Rocky Mountains. *Bulletin of Canadian Petroleum Geology*, v.18(3), pp.332-406.
- DeCelles, P. G., and Giles, K. A. (1996). Foreland basin systems. *Basin research*, v.8(2), pp.105-123.
- Decelles, P. G., and Hertel, F. (1989). Petrology of fluvial sands from the Amazonian foreland basin, Peru and Bolivia. *Geological Society of America Bulletin*, v.101(12), pp.1552-1562.
- Dubey, A. K. (2014). Understanding an orogenic belt. Springer, Heidelberg, New York, Dordrecht, London.p.401.

- Dubey, A. K., Bhakuni, S. S., and Selokar, A. D. (2004). Structural evolution of the Kangra recess, Himachal Himalaya: a model based on magnetic and petrofabric strains. *Journal of Asian Earth Sciences*, v.24(2), pp.245-258.
- Einsele, G. (2013). *Sedimentary basins: evolution, facies, and sediment budget*. Springer Science & Business Media, p.792.
- Erhardter, G. H., and Palzer-Khomenko, M. (2018). DiGeo: Introduction and a new tutorial to geological maps with QGIS 3. X. *Austrian Journal of Earth Sciences*, v.111(2), pp.223-224.
- Ghosh, D., Sinha, K.K., Sharma, B.C. and Kothari, P.K. (2017). Annual report for field season 2016-17. Unpublished Annual Report of Siwalik Investigations, NR, AMD, submitted to AMD, Hyderabad.
- Hassan, S. M., Mahmoud, A. A. A., and El-Mahdy, M. El kazzaz, YA (2014). Automated, manual lineaments extraction and geospatial analysis using remote sensing techniques and GIS, Case Study: Gabal Shabrawet area, South Ismailia, Egypt. *Australian Journal of Basic and Applied Sciences*, v.8(10), pp.110-120.
- Johnson, N. M., Stix, J., Tauxe, L., Cervený, P. F., and Tahirkheli, R. A. (1985). Paleomagnetic chronology, fluvial processes, and tectonic implications of the Siwalik deposits near Chinji village, Pakistan. *The Journal of Geology*, v.93(1), pp.27-40.
- Kaul, R., Umamaheshwar, K., Chandrasekaram, S., Deshmukh, R.D., Swarnkar, B.M., (1993). Uranium mineralization in the Siwalik of North Western, Himalaya. India. *J. Geol. Soc. India*, v.41, pp.243–258.
- Kothari, P.K. (2018). Annual Report for field season 2017-18. Unpublished Annual Report of Siwalik Investigations NR, AMD, submitted to AMD, Hyderabad.p.102.
- Kothari, P.K., Sinha, K.K., Gupta, C. S., Ghosh, D., Rahaman, Md. M. and Sharma, B. C. (2017). Annual report for field season 2016-17. Unpublished Annual Report of Siwalik Investigations, NR, AMD, submitted to AMD, Hyderabad.p.71.
- Kothari, P.K., Sinha, K.K., Gupta, C. S., Ghosh, D., Bhattacharya, S.. and Sharma, B. C. (2019). Brief Annual report for field season 2018-19. Unpublished Brief Annual Report of Siwalik Investigations, NR, AMD, submitted to AMD, Hyderabad.p.91.

- Krishna, R. R., Kishan, D., and Sarup, J. (2015). Lineament extraction and lineament density assessment of Omkareshwar, MP, India, using GIS Techniques. *International Journal of Engineering and Management Research (IJEMR)*, v.5(3), pp.717-720.
- Kroonenberg SB (1994) Effects of provenance, sorting and weathering on the geochemistry of fluvial sands from different tectonic and climatic environments. *Proceedings of the 29th International Geological Congress, Part A. Kyoto, Japan*, pp.69–81.
- Kumar, R., Ghosh, S. K., and Sangode, S. J. (2003). Mio-Pliocene sedimentation history in the northwestern part of the Himalayan foreland basin, India. *Current Science*, pp.1006-1013.
- Kundu, A., Matin, A., and Eriksson, P. G. (2016). Petrography and geochemistry of the Middle Siwalik sandstones (tertiary) in understanding the provenance of sub-Himalayan sediments in the Lish River Valley, West Bengal, India. *Arabian Journal of Geosciences*, v.9(2),162.p.18.
- Leach, D. L., Viets, J. G., and Rowan, L. (1984). Appalachian-Ouachita orogeny and Mississippi Valley-type lead-zinc deposits. *Geological Society of America Abstracts with Programs (Vol. 16)*, p. 572.
- Malik, J. N., and Mohanty, C. (2007). Active tectonic influence on the evolution of drainage and landscape: geomorphic signatures from frontal and hinterland areas along the northwestern Himalaya, India. *Journal of Asian Earth Sciences*, v.29(5-6), pp. 604-618.
- Maynard JB, Valloni R, Yu HS (1982) Composition of modern deep sea sands from arc related basins. *Geol Soc Spec Publ*, v.10. pp.551–561.
- McNaught, M. A., & Mitra, G. (1993). A kinematic model for the origin of footwall synclines. *Journal of Structural Geology*, v.15(6), pp.805-808.
- Medlicott, H.B. (1865). On the geological structure and relations of the southern portion of the Himalayan ranges between the rivers Ganges and Ravee. *Mem. geol. Surv. India*, v.3 (2), pp.1-206.
- Miall, A. D. (2000). *Principles of sedimentary basin analysis*. Springer, p.616
- Moghal, M. Y. (2001). Current uranium activities in Pakistan (No. IAEA-TECDOC--1258). IAEA. pp.101-115.

- Oliver, J. (1986). Fluids expelled tectonically from orogenic belts: Their role in hydrocarbon migration and other geologic phenomena. *Geology*, v.14(2), pp. 99-102.
- Osterwald, F. W., and Dean, B. G. (1961). Relation of uranium deposits to tectonic pattern of the central Cordilleran foreland (No. 1087). US Government Printing Office, pp.337-390.
- Pascoe, E. H. (1964). *A Manual of the Geology of India and Burma*, vol. 3. Government of India Press, Calcutta, pp.1345-2130.
- Pilgrim, G. E. (1910). Preliminary note on a revised classification of the Tertiary freshwater deposits of India. *Records of the Geological Survey of India*, v.40, pp.185-205.
- Pilgrim, G. E. (1913). Correlation of the Siwalik with Mammal Horizon of Europe. *Records of the Geological Survey of India*, v.24(2), pp.1-129.
- Powers, P. M., Lillie, R. J., and Yeats, R. S. (1998). Structure and shortening of the Kangra and Dehra Dun reentrants, sub-Himalaya, India. *Geological Society of America Bulletin*, v.110(8), pp. 1010-1027.
- Rahaman, Md. M., Sharma, B. C. and Gupta, C. S. (2017). Annual report for field season 2016-17. Unpublished Annual Report of Siwalik Investigations, NR, AMD, submitted to AMD, Hyderabad.
- Raiverman, V., Srivastava, A. K., and Prasad, D. N. (1993). On the foothill thrust of northwestern Himalaya. *Journal of Himalayan Geology*, v.4(2), pp.237-256.
- Raiverman, V., Srivastava, A. K., and Prasad, D. N. (1994). Structural style in northwestern Himalayan foothills. *Him. Geol.* v.15. pp.263-280.
- Raiverman, V. (2002). Foreland sedimentation in Himalayan tectonic regime. A relook at the orogenic process. Bishen Singh Mahendra Pal Singh Publication, Dehradun. p.371.
- Ranjan N, Banerjee DM (2009) Central Himalayan crystallines as the primary source for the sandstone-shale suites of the Siwalik group: new geochemical evidence. *Gondwana Res*, v.16, pp.687–696.
- Roser BP, Korsch RJ (1986) Determination of tectonic setting of sandstone-mudstone suites using SiO₂ content and K₂O Na₂O ratio. *J Geol*, v.9, pp.635–650.

- Sangode, S. J. (1996). Magnetic polarity stratigraphy; the Siwalik sequence of Haripur area (HP), NW Himalaya. *J. Geol. Soc. India*, v.47, pp.683-704.
- Schwab, F.L. (1986) Sedimentary "signatures" offoreland basin assemblages: real or counterfeit? In: Allen PA, Homewood P (eds) *Foreland basins*. Int. Assoc. Sedimentologists Spec Publ, v.8, Blackwell, Oxford, pp. 395-410.
- Sinha S, Islam R, Ghosh SK, Kumar R, Sangode J (2007) Geochemistry of Neogene Siwalik mudstones along Punjab re-entrant, India: implications for source-area weathering, provenance and tectonic setting. *Curr Sci India*, v.92, pp. 1103–1113.
- Takorabt, M., Toubal, A. C., Haddoum, H., and Zerrouk, S. (2018). Determining the role of lineaments in underground hydrodynamics using Landsat 7 ETM+ data, case of the Chott El Gharbi Basin (western Algeria). *Arabian Journal of Geosciences*, v.11(4), pp.76.
- Tandon, S. K., Kumar, R., Koyama, M., and Niitsuma, N. (1984). Magnetic polarity stratigraphy of the Upper Siwalik subgroup, east of Chandigarh, Punjab sub-Himalaya, India. *J. Geol. Soc. India*, v.25(1), pp.45-55.
- Valdiya, K. S. (1977). Structural set-up of the Kumaun Lesser Himalaya. C, Jest (ed.), *Himalaya : Sciences de la Terre, Colloq. Int. C.N.R.S.*, v.268, pp. 449-462.
- Valdiya, K. S. (1980). The two intracrustal boundary thrusts of the Himalaya. *Tectonophysics*, v.66(4), pp.323-348.
- Valdiya, K. S., Joshi, D. D., Sanwal, R., and Tandon, S. K. (1984). Geomorphologic development across the active main boundary thrust, an example from the Nainital Hills in Kumaun Himalaya. *Journal of the Geological Society of India*, v.25(12), pp.761-774.
- Valdiya, K. S. (1989). Trans-Himadri intracrustal fault and basement upwarps. *Tectonics of the Western Himalaya*, v.232, pp.153-168.
- Veerawamy, K., Sharana, B., Naidu, D., and Harinarayana, T. (2010). Electrical structure across lesser and higher NW Himalaya, India. *Chinese Journal of Geophysics*, v.53(3), pp.576-584.
- Wyborn, L. A. I., Heinrich, C. A., and Jaques, A. L. (1994). Australian Proterozoic mineral systems: essential ingredients and mappable criteria. *AusIMM Annual Conference (Vol. 1994)*, pp. 109-115.